S03120100-TRT10000
ORNL/LTR-2022/5

Oak Ridge National Laboratory CINDER90 and CINDER2008 Comparison for Second Target Station Analysis

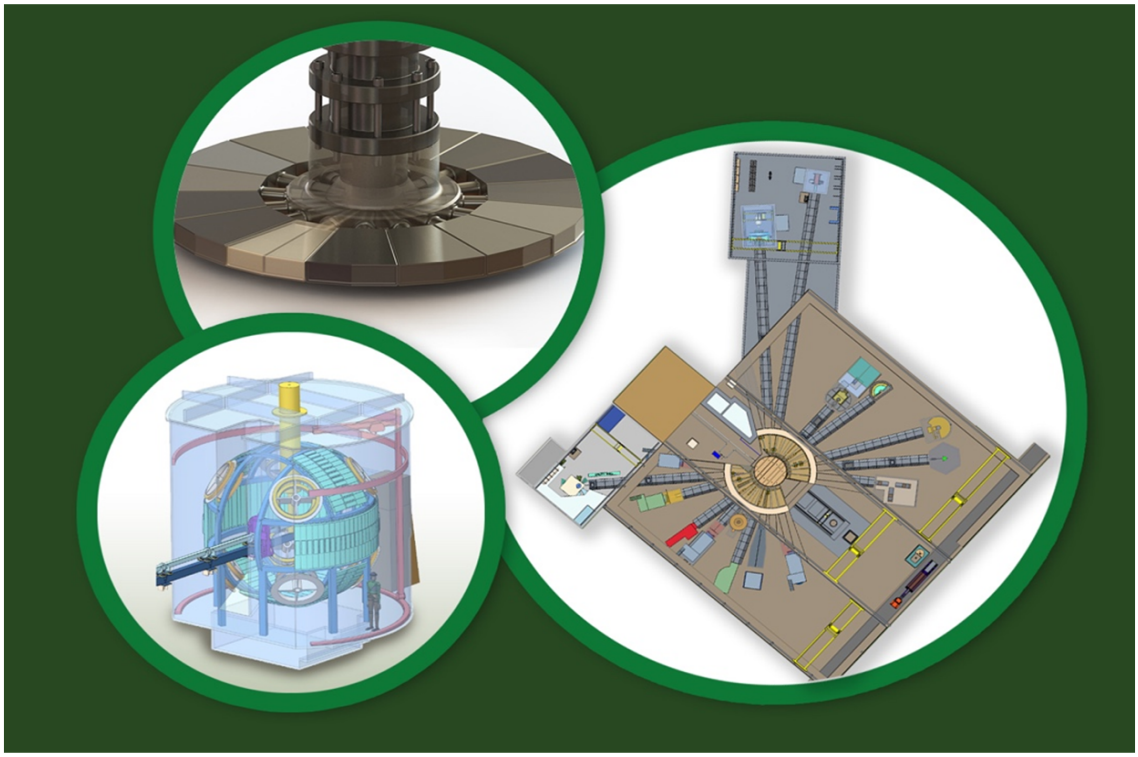

Tucker McClanahan, Ph.D.
Igor Remec, Ph.D.

May 2022

Approved for public release.
Distribution is unlimited.

OAK RIDGE National Laboratory

ORNL IS MANAGED BY UT-BATTELLE LLC FOR THE US DEPARTMENT OF ENERGY

S03120100-TRT10000
ORNL/LTR-2022/5

Second Target Station Project

CINDER90 and CINDER2008 Comparison for Second Target Station Analysis

Tucker McClanahan, Ph.D.
Igor Remec, Ph.D.

May 2022

Prepared by
OAK RIDGE NATIONAL LABORATORY
Oak Ridge, TN 37831
managed by
UT-Battelle LLC
for the
US DEPARTMENT OF ENERGY
under contract DE-AC05-00OR22725

CINDER90 and CINDER2008 Comparison for STS Target

CINDER90 and CINDER2008 Comparison for Second Target Station Analysis

LABORATORY ORNL	DIVISION/GROUP Second Target Station (STS) Project	CALC NO. S03120100-TRT10000
Prepared by Tucker McClanahan, Ph.D.	Level III Manager Igor Remec, Ph.D.	Lead Engineer

Other WBS elements affected:

Signature/Date

	REV 0	REV 1	REV 2	REV 3
Prepared By				
Task Leader				
Level III Manager				
Checked By				
Lead Engineer				

CONTENTS

LIST OF FIGURES

LIST OF TABLES

ABBREVIATIONS

ORNL	Oak Ridge National Laboratory
SNS	Spallation Neutron Source
STS	Second Target Station

EXECUTIVE SUMMARY

A preliminary target activation analysis for the Second Target Station (STS) at the Spallation Neutron Source (SNS) located at Oak Ridge National Laboratory (ORNL) was preformed using Monte Carlo N-Particle X (MCNPX), CINDER90, and the corresponding multi-group cross section libraries distributed with CINDER90. This preliminary analysis has been used to guide some design decisions of the STS target design. Using the MCNPX output files from this preliminary analysis, a comparison of the activation analysis using CINDER90 and CINDER2008 was performed. While the CINDER90 code has been validated for use in spallation source activation and transmutation calculations, and compares well with measurements, the transition to the modernized version of the code (CINDER2008) and the updated cross section libraries is desirable. The goal of this comparison is to evaluate the differences and implications for the STS activation analysis. Overall, the total activity differs between CINDER2008 and CINDER90 by no more than 20% for the materials evaluated in this report. The largest discrepancies were observed in the decay gamma intensity densities with CINDER90 calculating a factor of 2 higher than CINDER2008.

1 SCOPE

A preliminary target activation analysis for the Second Target Station (STS) at the Spallation Neutron Source (SNS) located at Oak Ridge National Laboratory (ORNL) was preformed using MCNPX, CINDER90, and the corresponding multi-group cross section libraries distributed with CINDER90. This preliminary analysis has been used to guide some design decisions of the STS target design. Using the MCNPX output files from this preliminary analysis, a comparison of the activation analysis using CINDER90 and CINDER2008 is necessary to justify the usage of CINDER2008 for future activation and transmutation analysis for the STS. The goal of the comparison is to see how well the results using the updated CINDER2008 transmutation code and the corresponding cross section libraries compare with the historical CINDER90 results. The CINDER90 code has been validated for use in spallation source activation and transmutation calculations and compares well with measurements [2, 3, 4, 5, 6, 7].

This report details the comparison between CINDER90 and CINDER2008 including a discussion of some cross section variations between the two cross section libraries that lead to the over estimation of a key isotope in spallation target shut down dose rates. A discussion of a bug in CINDER90 that allows the amount of time steps to affect the calculation of shutdown dose rates by prematurely truncating key transmutation paths and an example is given.

2 ASSUMPTIONS AND LIMITATIONS

The underlying neutron fluxes and spallation products are the same in all of the CINDER2008 and CINDER90 calculations. The differences observed in this study are due to changes in the CINDER code itself and the corresponding cross section sets. The comparison of the two versions of CINDER are only valid for the materials evaluated within this report.

3 METHODOLOGY AND MODELS

The details of the MCNP and CINDER calculations are discussed in detail in this section. The activation and transmutation calculations use versions of CINDER from the AARE V1.0 and CINDER/1.0.5 code packages available through RSICC. The AARE package includes the CINDER2008 code and CINDER/1.0.5 includes the CINDER90 code. Monte Carlo N-Particle X (MCNPX) code is a Monte Carlo based radiation transport code that is used to transport the source protons through the geometry and track the secondary, tertiary, etc. particles as they move and interact in the geometry [8]. The neutron fluxes and materials are relayed to the CINDER executables using the Activation script that comes as a part of the CINDER/1.0.5 and AARE packages. The results of the CINDER calculations are further processed by a Python script to produce the analysis discussed in this report. Sections 3.1, 3.2 & 3.3 provide a brief description of the model used in the MCNP calculation detailing the geometry, source, and how the neutron fluxes are tallied in the calculation. Section 3.4 details the activation and transmutation calculations used in the comparison and Section 3.5 describes the details of the irradiation periods by discussing the time step structure and the neutron flux weighting. Section 3.6 discusses the post-processing Python script used to evaluate the comparison between CINDER2008 and CINDER90.

3.1 GEOMETRY

The full target model is used as the geometry in the MCNP simulations. The target model is shown in Figure 1 where the bulk materials are called out and a scale is provided around the figure. The proton beam in Figure 1 is pointed up from the bottom of the figure. The 21 segments of the target are shown in the plan view. The position-averaged activation and transmutation of the parts a target segment are used in the comparison discussed in this report.

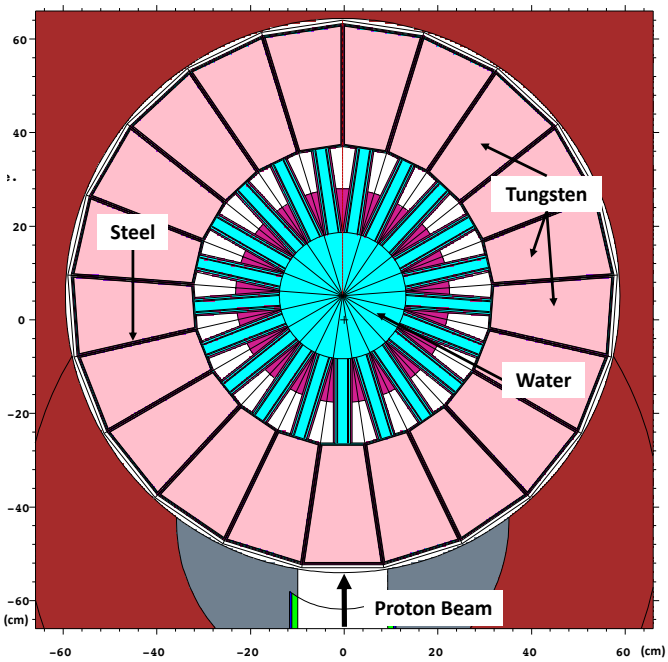

Figure 1. Plan view of the target geometry where the scales that surround the figure are in units of cm

Figure 2 shows a cross section view of the target geometry along the center of the proton beam axis. The proton beam in Figure 2 is coming from the left of the figure going to the right.

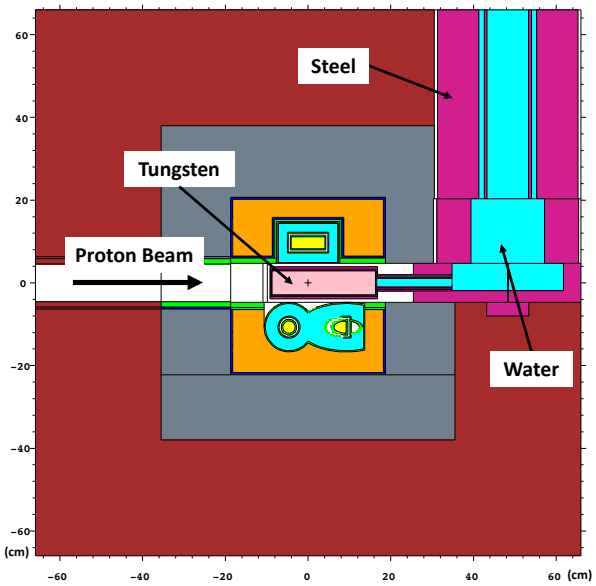

Figure 2. Cross section view of the target geometry where the scales that surround the figure are in units of cm

Figure 3 shows a more detailed cross section view of the geometry along the proton beam axis. The steel, tantalum, and tungsten labels point to the position of the MCNP cells that are used in the activation and transmutation comparisons.

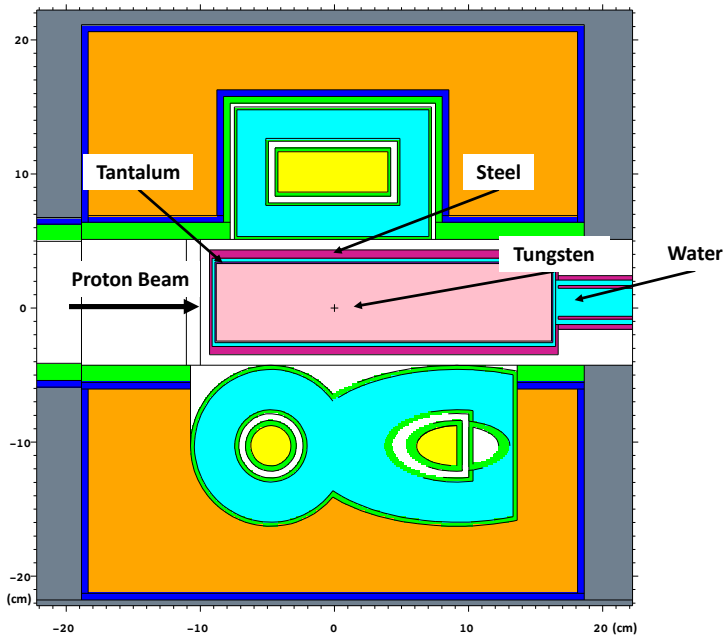

Figure 3. Detailed cross section view of the target geometry where the scales that surround the figure are in units of cm and the materials used in the activation and transportation comparison are shown.

3.2 SOURCES

The proton source used in the MCNP model is a mono-energetic 1.3 GeV proton beam with a double Gaussian distribution on the footprint perpendicular to the beam direction. The proton source starts just upstream of the proton beam window some 2.3 m upstream of the target, and has a beam profile with a height of 7 cm and a width of 11 cm.

3.3 TALLIES

The tallies used in the MCNP model are volume-averaged flux tallies over the regions of each individual segment of the target where one tally includes a single part of the model. Each tally encompasses a single material and the neutron fluxes are binned in energy.

3.4 TRANSMUTATION MECHANICS

Each of the code packages, AARE and CINDER/1.0.5, include an *Activation* script that facilitates the pre-processing of the MCNPX output files and the execution of CINDER for the various MCNP cells that may be included in the analysis. These *Activation* scripts also post-process the results of the CINDER calculations. The results of the CINDER calculations are further processed by a Python script to produce the analysis discussed in this report. Transmutation and activation in each part of each target segment is calculated by CINDER2008 and CINDER90 facilitated by the respective *Activation* scripts.

3.5 IRRADIATION SETUP

The time step structure used in both CINDER90 and CINDER2008 calculations consists of a period of 5000 hours of "beam on" followed by 3760 hours of "beam off" (decay), and that sequence is repeated 10 times to simulate a 10-year operation period. The "beam on" nomenclature stems from the CINDER manuals and is used to describe the time steps when the proton beam is impinging on the target. During "beam off" time steps, the neutron fluxes are set to 0 and the decay of the radionuclide is tracked. The 10-year operation period is then followed by several decay steps to estimate shut down quantities of interest out to 10 years. This report focuses on two times: the instant after the 10-year operation period and 10 years of decay after the original 10 years of operation.

3.6 POST-PROCESSING

The Python post-processing script is used to generate a position-averaged transmutation and activation of a part of a segment of the target. This approach assumes that a given segment of target spends the same amount of time in all target positions. During operation, the target is rotating in sync with the proton beam pulse. Therefore, each segment of the target will spend the same amount of time in each location around the target wheel.

After the results from the various CINDER runs are loaded and combined to generate the position-averaged quantities, the results are sorted and plotted. The quantities used in this report to compare CINDER90 and CINDER2008 are the activity, decay power, and overall gamma emission spectrum from each part. These quantities are compared via ratios, scatter plots of ratios, and several tables showing the top contributors to a specific quantity of interest. These quantities were selected because they are important for the design and safety analyses. These tables and figures are discussed in detail in Section 4.

An additional quantity of interest is the hazard categorization of the facility. Department of Energy (DOE) Standard DOE-STD-1027-2018 outlines the procedure for calculating the Sum Of Ratios (SOR) quantity and provides the threshold activity and mass quantities (TQs) for a number of hazardous radioisotopes [9]. The TQ is the activity limit for a specific radionuclide that if the facility in question has more than the TQ specified amount of radioisotopic activity, the facility will be categorized as the hazard class relating to the TQ amount. The SOR value determines the categorization of the facility when using either category 2 (HC-2) or category 3 (HC-3) threshold activity values. The DOE Standard states, "If the SOR is greater than or equal to a value of 1.0, the facility shall be initially categorized as HC-2 or HC-3 depending upon the TQs used in the calculation." The TQs provided in the standard are applied to the activities calculated by CINDER90 and CINDER2008, and to calculate the ratio for each isotope and the ratios are summed over all isotopes to obtain the SOR values.

3.7 CINDER OPTIONS

The options used to calculate the transmutation of the target systems are confirmed to be equivalent between the CINDER90 and CINDER2008 runs. Table 1 shows the CINDER options used in the analysis discussed in this document along with brief descriptions from the CINDER manuals about each CINDER option. The *TST* parameter is set to a value of 1E-4 which is different from the default value of 1E-12 in order to match the original CINDER90 activation calculations. The number of title lines as set by the *NLINTL* parameter is set to 2 whereas the default is 0 but this will not alter the results of the analysis. All of the other CINDER options are the defaults.

Table 1. CINDER Run Options

Option	Value	Description
TST	1E-4	Parameter used in justifying termination of chains based on activity.
SIGNIF	1E-12	Parameter used in justifying termination of chains based on atom density.
EPSM	100*ESPN	The value for x of $\exp(-x)$ below which $\exp(-x)$ is set to unity and $(1 - \exp(-x))$ is set to x. An input epsm value smaller than 100*epsn is reset in the code to 100×epsn
EPSN	Machine Precision	The reciprocal of a power of 10 having exponent not exceeding the number of significant digits guaranteed by the computer stored word.
EXPONMAX	Machine Parameter	The maximum exponent, positive or negative, guaranteed by the computer.
KABC	0	No longer used
KCHN	0	Flag to request writing of chains edit file. < 0 = -AZS, only the chains contributing to the nuclide identified by AZS are output. 0 = no chains written 1 = all chains written
KLIB	0	Flag to request writing of libcheck edit file. 0: no, 1: yes
NFE	0	Parameter identifying the selection of fission-product yields appropriate for the neutron flux spectrum of this problem. 0=none, 1=thermal, 2=fast, 3=high energy
LTSDNZ	-1	Time-step of previous calculation from which the calculated nuclide inventory in the dnz file should be read and used as the initial inventory of the present calculation
NLINTL	2	Number of title lines to be used in post-processing routines. Its value should be one less than the number of lines of description.
NOSAME	0	Stop the evolution of a chain at its return to a nuclide appearing earlier in the chain. 0=no, 1=yes
RUSS	1	CINDER2008: No longer used. CINDER90: Suppress lines in TABCODE tables of all-zero values. [0=no, 1=yes, default=1]

4 ANALYSIS AND RESULTS

The results of the CINDER90 and CINDER2008 comparison are discussed in sections categorized by the quantity of interest. Section 4.1 discusses the comparison of the activity of a few parts of the target made from different materials, Section 4.2 describes how the decay power compares, and Section 4.3 discusses the hazard categorization comparison, and Section 4.4 discusses the decay gamma spectra comparison. Section 4.5 describes a discrepancy observed in ^{148}Gd production. Section 4.6 presents a bug found in the CINDER90 code and provides an example of how the bug can manifest in the results of key isotopes.

4.1 ACTIVITY COMPARISON

The activity comparison of CINDER2008 and CINDER90 is separated by material. Section 4.1.1 discusses the activity results for a single tungsten target wedge, Section 4.1.2 shows the tantalum shell activity results, and Section 4.1.3 describes the activity produced in the steel layer around the tantalum shell.

4.1.1 Tungsten Wedge

The position-averaged activity for a single tungsten wedge over time for both CINDER2008 and CINDER90 is shown in Figure 4. Activities are calculated at the specific time shown on the x-axis and the points are connected using linear interpolation. Figure 4a shows the raw CINDER2008 and CINDER90 activities over time and Figure 4b shows the ratio of the CINDER2008 results over the CINDER90 results. During the 10 years of target operation, the greatest discrepancies between CINDER90 and CINDER2008 are observed at the end of each beam-on period, when the differences reach almost 25%, while at the ends of the beam-on periods, the activities agree to better than 5%. During the decay period following the 10 years of operation, the activities from both codes agree to better than 5%.

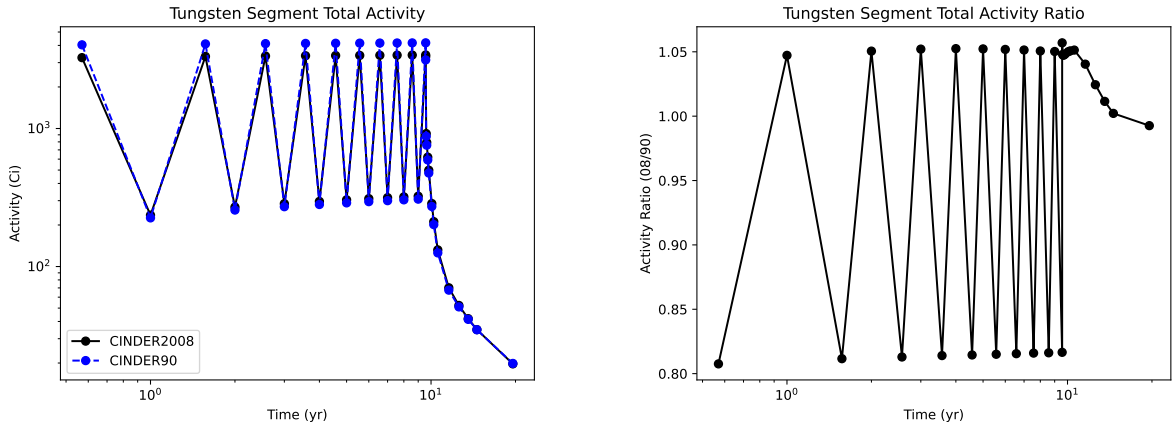

(a) CINDER2008 and CINDER90 activity over time. **(b) Ratio of CINDER2008 and CINDER90 activity.**

Figure 4. Position-averaged activity for a single tungsten target wedge over time.

The position-averaged activity for a single tungsten wedge after 10 years of operation as calculated by CINDER2008 and CINDER 90 is shown in Table 2. The activities shown in Table 2 are at the instant in time when the beam turns off with no decay period, and these radionuclides would be extremely difficult to verify at this time step. This time step is chosen because this is the instant where the largest discrepancies between CINDER90 and CINDER2008 are likely to manifest. The top 10 highest contributors to the activity including a sum of the activity of these top ten so that one can observe how much these top ten contributors account for the total activity. Overall, CINDER90 calculates a 20% higher total activity than CINDER2008. There are some key differences in the activity of isotopes that contribute more than 1% to the overall activity. CINDER90 calculates a factor of 25 higher activity in ^{183m}W than CINDER2008. However, ^{183m}W has a half life of 5 seconds and would quickly decay away after shutdown. The total activity and many of the radionuclides that contribute more than 1% to the total activity are within 20% of agreement.

Table 2. Tungsten Wedge Activity Contributions after 10 years Operation

Rank	CINDER90 Isotope	CINDER90 Activity (Ci)	Percent of Total	CINDER2008 Isotope	CINDER2008 Activity (Ci)	Percent of Total
1	^{187}W	1.2282E+03	29.4131	^{187}W	1.3574E+03	39.8133
2	^{183m}W	9.7538E+02	23.3595	^{185}W	5.9494E+02	17.4499
3	^{185}W	5.6438E+02	13.5164	^{181}W	1.4131E+02	4.1447
4	^{181}W	1.4080E+02	3.3721	^{179}W	5.3467E+01	1.5682
5	^{179}W	5.3467E+01	1.2805	^{178}Ta	4.8774E+01	1.4306
6	^{178}Ta	4.8773E+01	1.1681	^{179}Ta	4.3968E+01	1.2896
7	^{179}Ta	4.3227E+01	1.0352	^{178}W	3.9359E+01	1.1544
8	^{178}W	3.9358E+01	0.9426	^{183m}W	3.8656E+01	1.1338
9	^{177}Ta	3.8603E+01	0.9245	^{177}Ta	3.8603E+01	1.1323
10	^{185m}W	3.4130E+01	0.8174	^{3}H	3.0002E+01	0.8800
Top 10 Total		3.1663E+03	75.8294		2.3865E+03	69.9968
Total Activity		4.1755E+03			3.4094E+03	

Table 3 shows the position-averaged activity for a single tungsten wedge after 10 years of operation followed by an additional 10 years of shut-down. The magnitude of differences in total activity are much lower after 10 years of decay. The total activities are within 0.7% of each other. Of the isotopes that contribute more than 1% to the total activity, ^{179}Ta has the largest differences between CINDER90 and CINDER2008 with CINDER90 calculating 62% more than CINDER2008.

Table 3. Tungsten Wedge Activity Contributions after 10 years of Shut-Down

Rank	CINDER90 Isotope	CINDER90 Activity (Ci)	Percent of Total	CINDER2008 Isotope	CINDER2008 Activity (Ci)	Percent of Total
1	^{3}H	1.7095E+01	86.0803	^{3}H	1.7095E+01	86.7215
2	^{179}Ta	9.5944E-01	4.8313	^{179}Ta	5.9332E-01	3.0099
3	^{145}Pm	5.3188E-01	2.6783	^{145}Pm	5.2026E-01	2.6392
4	^{133}Ba	2.9796E-01	1.5004	^{133}Ba	2.9816E-01	1.5126
5	^{172}Lu	2.2331E-01	1.1245	^{172}Lu	2.2353E-01	1.1339
6	^{172}Hf	2.2110E-01	1.1134	^{172}Hf	2.2132E-01	1.1227
7	^{148}Gd	1.7552E-01	0.8838	^{172m}Lu	2.2132E-01	1.1227
8	^{157}Tb	1.1841E-01	0.5962	^{157}Tb	1.7331E-01	0.8792
9	^{173}Lu	8.6924E-02	0.4377	^{148}Gd	1.2209E-01	0.6194
10	^{174}Lu	7.3306E-02	0.3691	^{173}Lu	8.7227E-02	0.4425
Top 10 Total		1.9782E+01	99.6150		1.9555E+01	99.2037
Total Activity		1.9859E+01			1.9712E+01	

Figure 5 shows the ratio of activity calculated by CINDER2008 and CINDER90 for all radionuclides included in the comparison after 10 years of operation. Figure 6 shows the activity ratio following 10 years of decay. The color scale of Figures 5 & 6 indicates whether CINDER2008 calculates more activity of an isotope as a warmer color and if CINDER90 calculates more activity as a cooler color. Grey is used to indicate that the ratio is near to 1.0. Artificial limits of a factor of 10 either way are applied to the figure. For example, if the ratio is 100, it would be depicted as solid red and if the ratio is 0.0001, it would be depicted as solid blue. Figures 5 & 6 provide a comprehensive qualitative view of the CINDER2008 and CINDER90 activity comparison.

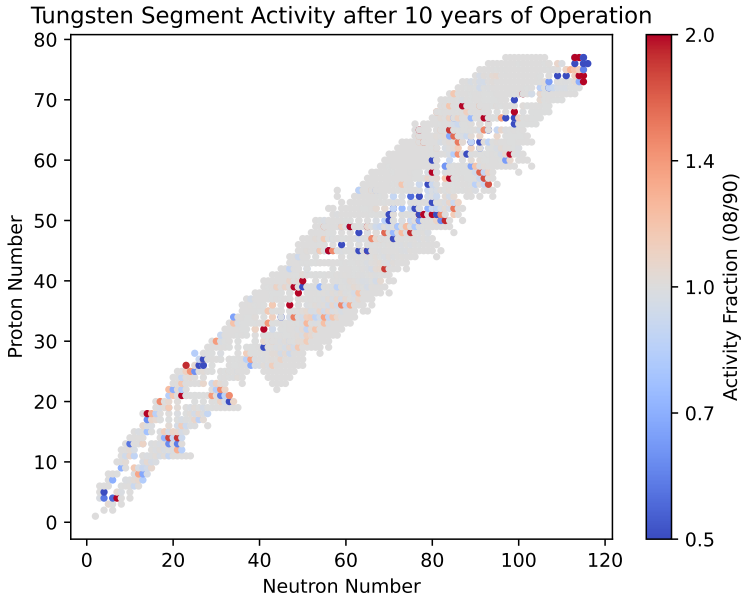

Figure 5. Isotopic distribution of the activity of a single tungsten wedge after 10 years of operation.

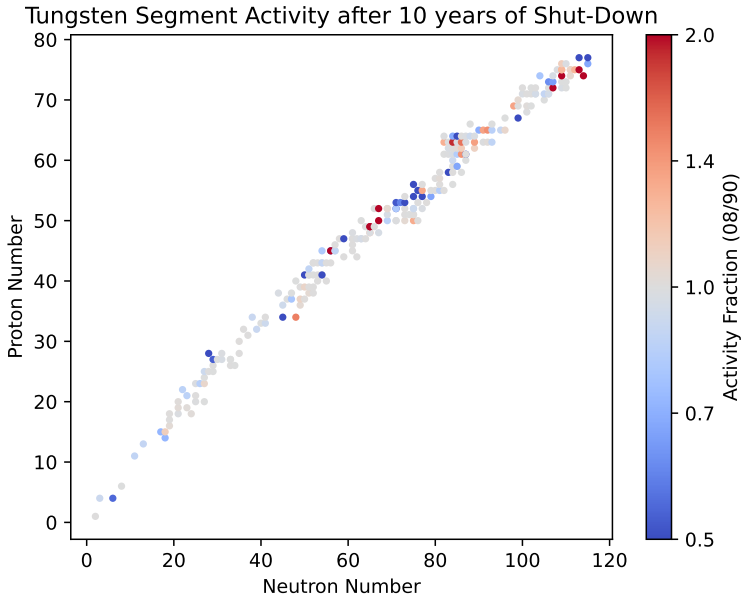

Figure 6. Isotopic distribution of the activity of a single tungsten wedge after 10 years of shut-down.

4.1.2 Tantalum Shell

Figure 7 shows the position-averaged activity for a tantalum shell of one target segment (one tungsten wedge) over time as calculated by CINDER2008 and CINDER90. The activity ratio, shown in Figure 7b, follows a similar trend as the tungsten target wedge activity except that the discrepancies are worse for the tantalum shell when the beam is on. When the beam is on, the discrepancies between CINDER90 and CINDER2008 reach values of >25%.

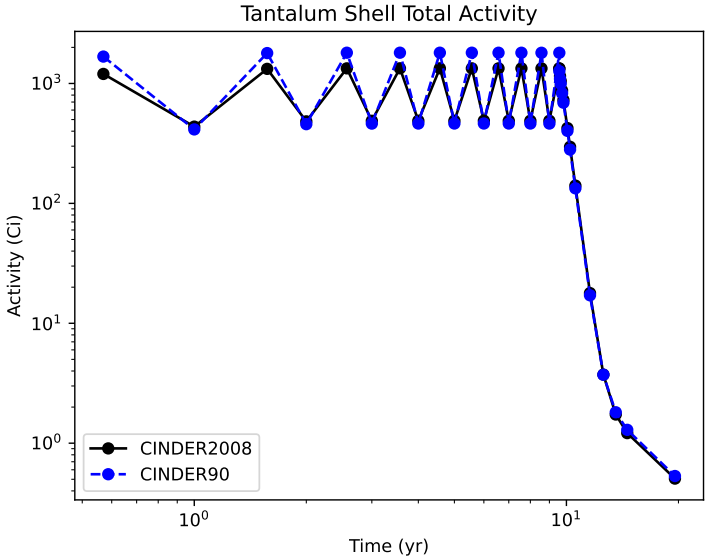

(a) CINDER2008 and CINDER90 activity over time.

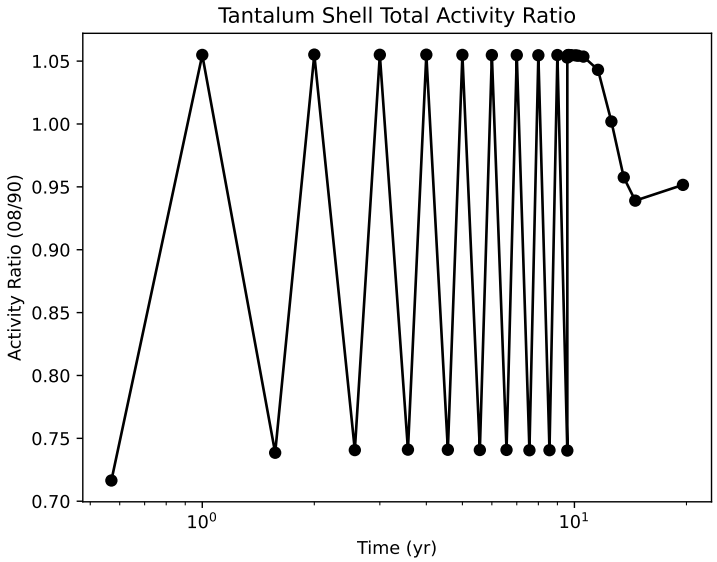

(b) Ratio of CINDER2008 and CINDER90 activity.

Figure 7. Position-averaged activity for a single tantalum shell over time.

Table 4 shows the top contributors to the activity at the time directly after 10 years of operation. The total activities differ by ~25% at this time step. Much of this discrepancy comes from ^{182m}Ta production. ^{182m}Ta is the second highest contributor to overall activity in the CINDER90 calculation but does not make it to the top 10 in the CINDER2008 calculation. The discrepancy with ^{182m}Ta is not concerning because ^{182m}Ta quickly decays with a half-life of 283 ms to ^{182}Ta and the activity of ^{182}Ta is much greater than the contribution to the activity from ^{182m}Ta in both CINDER2008 and CINDER90.

Table 4. Tantalum Shell Activity Contributions after 10 years Operation

Rank	**CINDER90 Isotope**	**CINDER90 Activity** (Ci)	**Percent of Total**	**CINDER2008 Isotope**	**CINDER2008 Activity** (Ci)	**Percent of Total**
1	^{182}Ta	1.1818E+03	65.5655	^{182}Ta	1.2467E+03	93.4109
2	^{182m}Ta	5.3493E+02	29.6783	^{183}Ta	4.2298E+01	3.1692
3	^{183}Ta	4.0846E+01	2.2661	^{180}Ta	8.1138E+00	0.6079
4	^{180}Ta	6.8444E+00	0.3797	^{179}Ta	3.6490E+00	0.2734
5	^{179}Ta	3.6981E+00	0.2052	^{177}Ta	2.2409E+00	0.1679
6	^{183m}W	2.5809E+00	0.1432	^{178}Ta	2.1694E+00	0.1625
7	^{177}Ta	2.2409E+00	0.1243	^{183m}W	2.1206E+00	0.1589
8	^{178}Ta	2.1694E+00	0.1204	^{175}Hf	1.2857E+00	0.0963
9	^{175}Hf	1.2834E+00	0.0712	^{176}Ta	1.1849E+00	0.0888
10	^{176}Ta	1.1849E+00	0.0657	^{175}Ta	1.0043E+00	0.0752
Top 10 Total		1.7776E+03	98.6197		1.3108E+03	98.2111
Total Activity		1.8024E+03			1.3347E+03	

Table 5 shows the top contributors to activity after 10 years of decay. CINDER2008 and CINDER90 total activities are ~5% different with CINDER90 calculating a more radioactive tantalum shell. There are some minor discrepancies in several individual isotopes that sum to the ~5% difference observed in the total.

Table 5. Tantalum Shell Activity Contributions after 10 years of Decay

Rank	CINDER90 Isotope	CINDER90 Activity (Ci)	Percent of Total	CINDER2008 Isotope	CINDER2008 Activity (Ci)	Percent of Total
1	^{3}H	3.9469E-01	74.1574	^{3}H	3.9463E-01	77.9120
2	^{179}Ta	8.2105E-02	15.4265	^{179}Ta	4.9242E-02	9.7219
3	^{145}Pm	1.2587E-02	2.3650	^{145}Pm	1.2306E-02	2.4297
4	^{172}Lu	7.5010E-03	1.4093	^{172}Lu	7.5086E-03	1.4824
5	^{133}Ba	7.4290E-03	1.3958	^{172}Hf	7.4350E-03	1.4679
6	^{172}Hf	7.4281E-03	1.3956	^{172m}Lu	7.4350E-03	1.4679
7	^{174}Lu	7.1636E-03	1.3459	^{133}Ba	7.4346E-03	1.4678
8	^{148}Gd	4.2305E-03	0.7949	^{174}Lu	7.1581E-03	1.4132
9	^{173}Lu	3.4698E-03	0.6519	^{157}Tb	4.1716E-03	0.8236
10	^{157}Tb	2.8489E-03	0.5353	^{173}Lu	3.4840E-03	0.6878
Top 10 Total		5.2946E-01	99.4776		5.0080E-01	98.8743
Total Activity		5.3224E-01			5.0651E-01	

Figures 8 & 9 show an overview of the CINDER2008 and CINDER90 ratios for all isotopes calculated for both directly after operation and after a 10-year decay period. CINDER90 predicted higher activities for many of the isotopes when compared with CINDER2008 for the tantalum shell as shown by the many cooler colors in Figure 8.

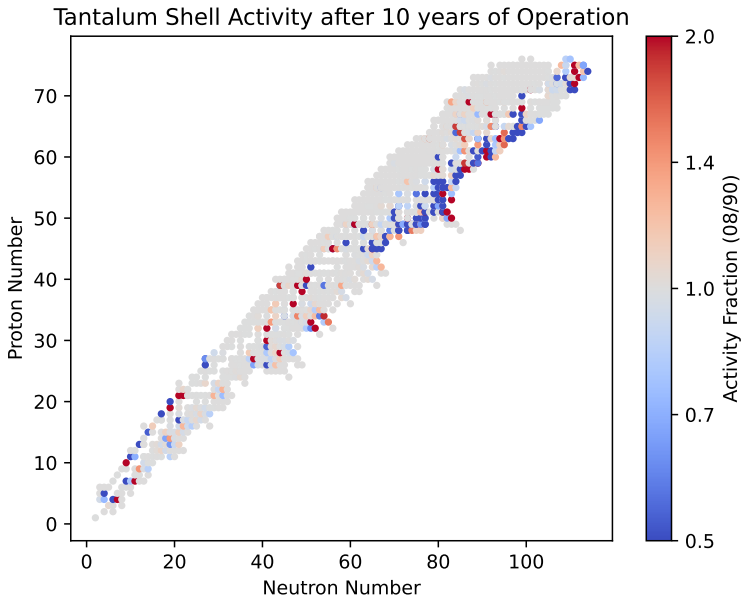

Figure 8. Isotopic distribution of the activity of a single tantalum shell after 10 years of operation.

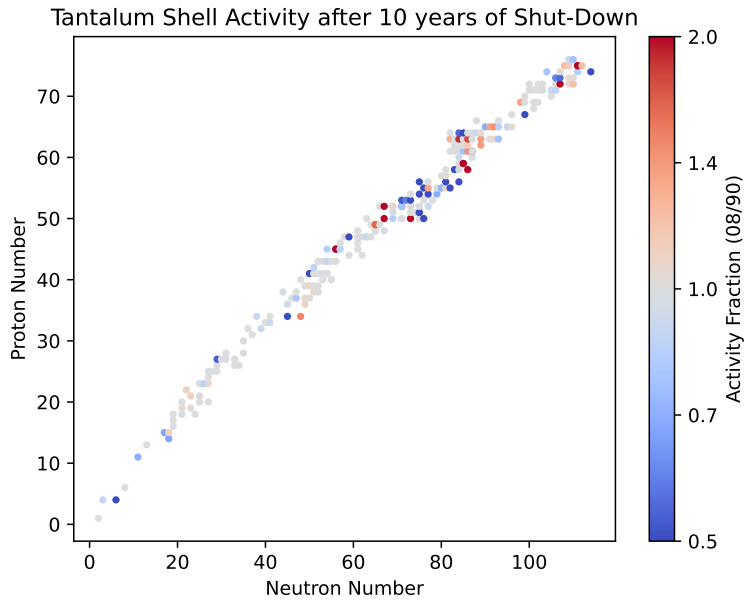

Figure 9. Isotopic distribution of the activity of a single tantalum shell after 10 years of shut-down.

4.1.3 Steel Layer

The steel layer referenced in this section is indicated in Figure 3 by the "Steel" notation. This layer of steel completely surrounds the tantalum shell and is located just outside the water coolant loop. This steel is the exterior-most material of the target and therefore the first target material irradiated by the proton beam. Figure 10a shows the total activity of the steel layer as a function of time where the activity can be seen to increase during the "beam on" periods and decrease during times of shut down as calculated by CINDER2008 and CINDER90. Figure 10b shows the ratio of CINDER2008 and CINDER90 activity over time. Overall, CINDER90 and CINDER2008 stay within 5% of each other over all time steps observed in the comparison. The two codes have the largest deviations at the end of the "beam on" periods.

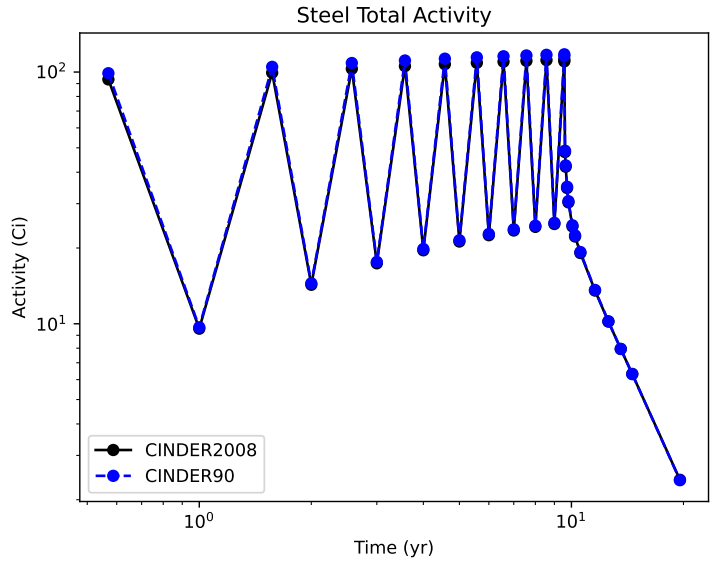

(a) CINDER2008 and CINDER90 activity over time.

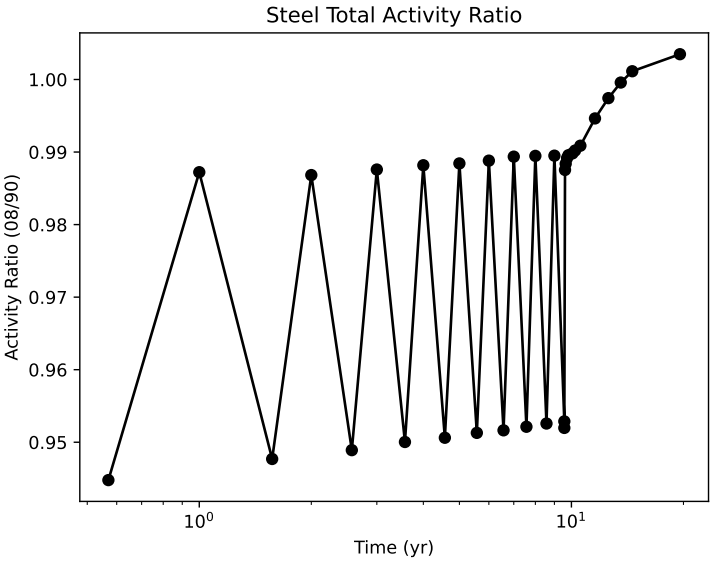

(b) Ratio of CINDER2008 and CINDER90 activity.

Figure 10. Position-averaged activity for a single steel layer over time.

Table 6 shows the top 10 contributors to the CINDER2008 and CINDER90 total activities for the time period directly after 10 years of operation. The total activities for CINDER2008 and CINDER90 are within 5% of each other. One notable difference between the two codes' top ten radionuclei is the absence of ^{58m}Co ($t_{1/2}$=8.9 hr) in the CINDER2008 top ten contributors list. The absence of ^{58m}Co is a result of some compounding factors: destruction paths in CINDER2008 cross sections that are not present in the CINDER90 cross sections, and the order of magnitude difference in the ^{58}Ni(n,p)^{58m}Co cross sections

between CINDER90 and CINDER2008. The cross section included in CINDER90 for ^{58}Ni(n,p)^{58m}Co is > 10 times higher than CINDER2008's cross section for incident neutron energies less than 10 MeV.

Table 6. Steel Layer Activity Contributions after 10 years of Operation

Rank	**CINDER90 Isotope**	**CINDER90 Activity** (Ci)	**Percent of Total**	**CINDER2008 Isotope**	**CINDER2008 Activity** (Ci)	**Percent of Total**
1	^{56}Mn	4.0581E+01	34.4916	^{56}Mn	3.9114E+01	34.8979
2	^{51}Cr	1.9867E+01	16.8859	^{51}Cr	1.9410E+01	17.3177
3	^{55}Fe	1.4556E+01	12.3722	^{55}Fe	1.4587E+01	13.0142
4	^{54}Mn	6.7096E+00	5.7028	^{54}Mn	6.1757E+00	5.5100
5	^{58}Co	5.2576E+00	4.4687	^{58}Co	5.3491E+00	4.7725
6	^{58m}Co	4.0970E+00	3.4822	^{60m}Co	4.1158E+00	3.6721
7	^{60m}Co	3.6453E+00	3.0983	^{60}Co	2.8998E+00	2.5872
8	^{60}Co	2.9019E+00	2.4664	^{57}Co	2.2366E+00	1.9955
9	^{57}Co	2.0953E+00	1.7809	^{49}V	1.6314E+00	1.4555
10	^{99}Mo	2.0731E+00	1.7620	^{99}Mo	1.5861E+00	1.4151
Top 10 Total		1.0178E+02	86.5111		9.7106E+01	86.6377
Total Activity		1.1765E+02			1.1208E+02	

Table 7 shows the top ten contributors to the total activity after 10 years of decay following the 10-year period of operation. Within the isotopes that contribute more than 1% to the total activity, CINDER2008 and CINDER90 agree to within 0.3%.

Table 7. Steel Activity Contributions after 10 years of Decay

Rank	CINDER90 Isotope	CINDER90 Activity (Ci)	Percent of Total	CINDER2008 Isotope	CINDER2008 Activity (Ci)	Percent of Total
1	^{55}Fe	1.1490E+00	48.0503	^{55}Fe	1.1592E+00	48.3070
2	^{60}Co	7.7911E-01	32.5804	^{60}Co	7.7844E-01	32.4407
3	^{63}Ni	2.3049E-01	9.6384	^{63}Ni	2.3237E-01	9.6838
4	^{3}H	2.1358E-01	8.9315	^{3}H	2.1418E-01	8.9259
5	^{93m}Nb	4.7801E-03	0.1999	^{93m}Nb	3.1858E-03	0.1328
6	^{59}Ni	2.1445E-03	0.0897	^{59}Ni	2.1673E-03	0.0903
7	^{54}Mn	2.0137E-03	0.0842	^{54}Mn	1.8541E-03	0.0773
8	^{22}Na	2.0078E-03	0.0840	^{44}Sc	1.5410E-03	0.0642
9	^{44}Sc	1.8682E-03	0.0781	^{44}Ti	1.5410E-03	0.0642
10	^{44}Ti	1.8682E-03	0.0781	^{39}Ar	1.1236E-03	0.0468
Top 10 Total		2.3869E+00	99.8147		2.3956E+00	99.8330
Total Activity		2.3913E+00			2.3996E+00	

Figure 12 shows an overview of all isotopes in each calculation and how they compare between CINDER2008 and CINDER90. CINDER2008 and CINDER90 closely agree on most isotopes both at the end of the 10-year period of operation and after the 10-year period of decay.

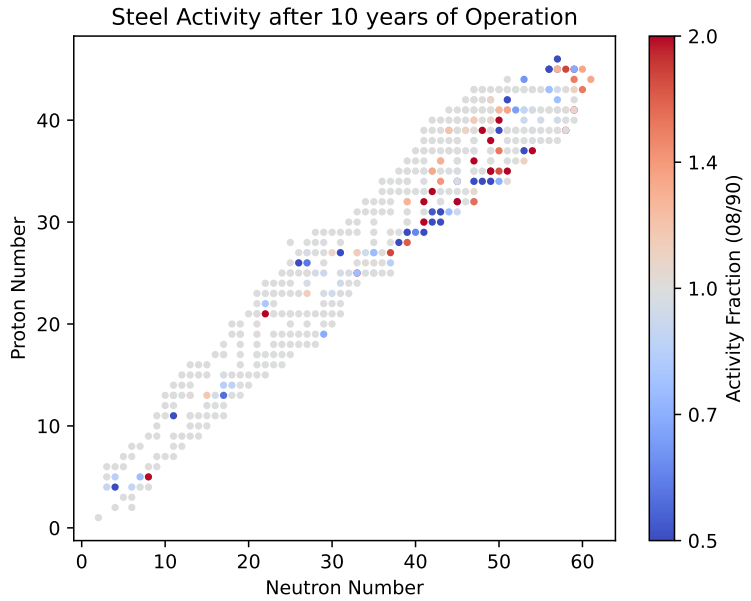

Figure 11. Isotopic distribution of the activity of a single steel layer after 10 years of operation.

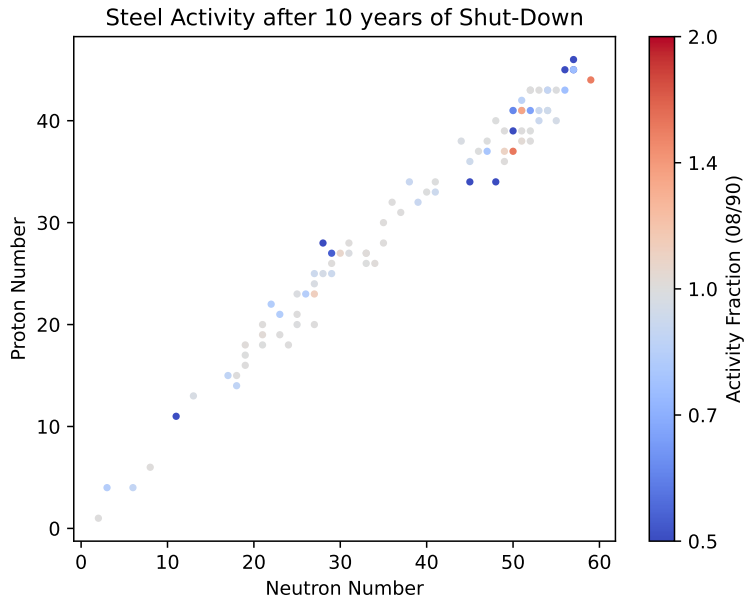

Figure 12. Isotopic distribution of the activity of a single steel layer after 10 years of shut-down.

4.2 DECAY POWER

The decay power results have been separated by material. Section 4.2.1 shows the results for a single tungsten wedge, Section 4.2.2 discusses the decay power results for a single tantalum shell, and Section 4.2.3 shows the steel layer decay power results. The decay power results, shown in the sections described below, is a metric that describes the amount of energy emitted per second by the radionuclides in the irradiated material. This decay power metric may be used to estimate decay heating loads for long-term waste disposal and storage.

4.2.1 Tungsten Wedge

Figure 13 shows the decay power over time for a single tungsten wedge and follows a similar trend with the tungsten wedge activity discussed in Section 4.1.1. Figure 13b shows the ratio of CINDER2008 and CINDER90 decay power results over time. The two calculations are within 10% of each other. The sudden change in the ratio of CINDER90 and CINDER2008 at 10 years is due to the short lived contribution of ^{183m}W to the CINDER90 decay power that is not present in the CINDER2008 calculation. This discrepancy is due to a change in the production cross sections between versions of CINDER.

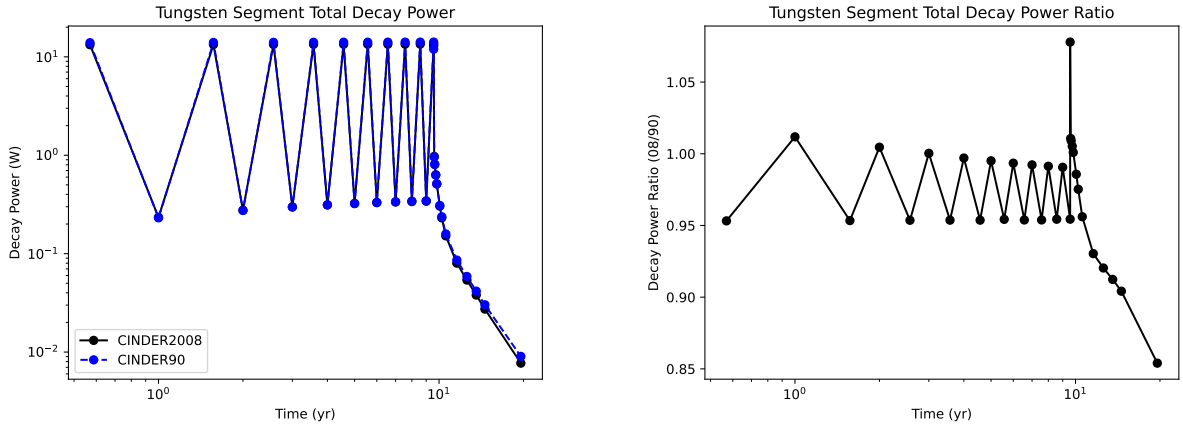

(a) CINDER2008 and CINDER90 decay power over time.

(b) Ratio of CINDER2008 and CINDER90 decay power.

Figure 13. Position-averaged decay power for a single tungsten target wedge over time.

Table 8 shows the top ten contributors to the decay power after 10 years of operation. One of the main discrepancies between CINDER90 and CINDER2008 top ten radionucides is the ^{183m}W decay power. ^{183m}W is one of the top contributors for CINDER90 but the discrepancy would be short lived as ^{183m}W has a 5.3 s half-life. Overall, CINDER2008 and CINDER90 are within 5% for total decay power.

Table 8. Tungsten Wedge Decay Power Contributions at 10 years of Operation

Rank	**CINDER90 Isotope**	**CINDER90** (W)	**Percent of Total**	**CINDER2008 Isotope**	**CINDER2008** (W)	**Percent of Total**
1	^{187}W	5.2562E+00	37.2207	^{187}W	5.9278E+00	43.9914
2	^{183m}W	1.7148E+00	12.1428	^{185}W	4.4780E-01	3.3232
3	^{185}W	4.2466E-01	3.0072	^{176}Ta	3.7827E-01	2.8072
4	^{176}Ta	3.8093E-01	2.6975	^{170}Lu	2.1869E-01	1.6230
5	^{170}Lu	2.1869E-01	1.5486	^{168}Lu	2.1109E-01	1.5665
6	^{168}Lu	2.1102E-01	1.4943	^{175}Ta	1.8732E-01	1.3902
7	^{171}Hf	1.6888E-01	1.1959	^{172}Lu	1.3315E-01	0.9881
8	^{172}Lu	1.4748E-01	1.0444	^{182}Ta	1.2775E-01	0.9481
9	^{177}W	1.3553E-01	0.9597	^{171}Hf	1.2641E-01	0.9381
10	^{172}Ta	1.3067E-01	0.9253	^{177}W	1.2318E-01	0.9142
Top 10 Total		8.7888E+00	62.2365		7.8815E+00	58.4898
Total Decay Power		1.4122E+01			1.3475E+01	

Table 9 shows the top contributors to decay power after 10 years of decay. Overall, CINDER2008 and CINDER90 agree to within 17% when comparing total decay power. There are some major discrepancies

between the two codes when comparing individual isotopes. CINDER90 calculates ~42% more ^{148}Gd than CINDER2008.

Table 9. Tungsten Wedge Decay Power Contributions at 10 years of Decay

Rank	CINDER90 Isotope	CINDER90 (W)	Percent of Total	CINDER2008 Isotope	CINDER2008 (W)	Percent of Total
1	^{148}Gd	3.4033E-03	37.6487	^{172}Lu	2.7203E-03	35.2397
2	^{172}Lu	3.0103E-03	33.3011	^{148}Gd	2.3673E-03	30.6671
3	^{133}Ba	8.0396E-04	8.8936	^{133}Ba	8.0258E-04	10.3971
4	^{3}H	5.7655E-04	6.3779	^{3}H	5.7663E-04	7.4699
5	^{172}Hf	2.7784E-04	3.0736	^{152}Eu	2.6531E-04	3.4370
6	^{152}Eu	1.9104E-04	2.1133	^{172}Hf	2.3354E-04	3.0254
7	^{179}Ta	1.8785E-04	2.0780	^{179}Ta	1.2890E-04	1.6698
8	^{145}Pm	1.3872E-04	1.5346	^{145}Pm	1.2604E-04	1.6328
9	^{173}Lu	1.0825E-04	1.1975	^{173}Lu	1.1568E-04	1.4986
10	^{174}Lu	7.4867E-05	0.8282	^{174}Lu	6.7526E-05	0.8748
Top 10 Total		8.7727E-03	97.0464		7.4037E-03	95.9120
Total Decay Power		9.0397E-03			7.7193E-03	

4.2.2 Tantalum Shell

Figure 14 shows the decay power over time for the tantalum shell. The ratio of CINDER2008 and CINDER 90 over time, shown in Figure 14b, does not have as much deviation between "beam on" and "beam off" as observed in the activity over time metric. The deviation grows between the two codes at longer decay times.

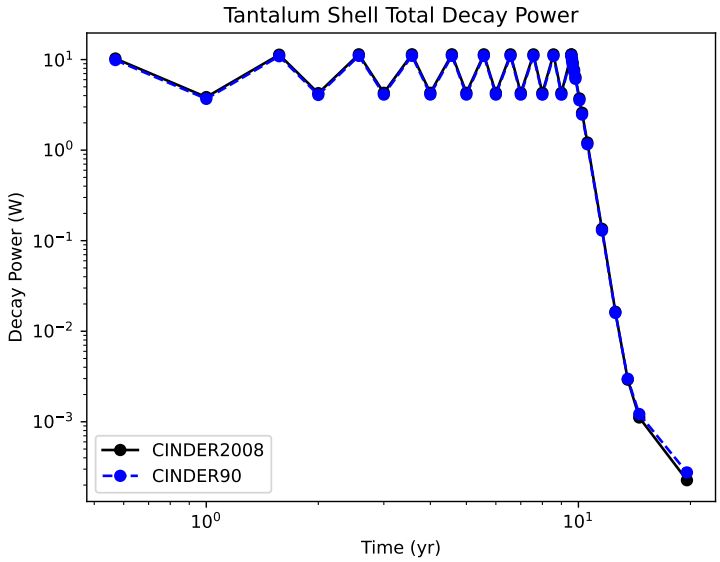

(a) CINDER2008 and CINDER90 decay power over time.

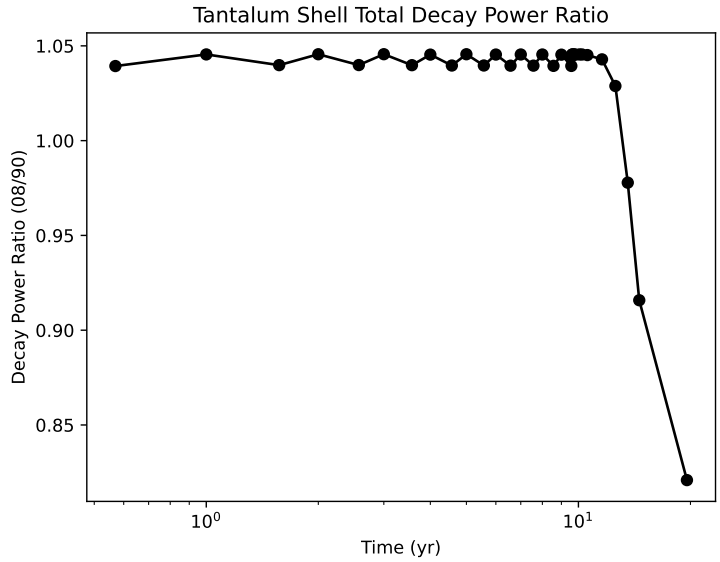

(b) Ratio of CINDER2008 and CINDER90 decay power.

Figure 14. Position-averaged decay power for a single tantalum shell over time.

Table 10 shows the top ten contributors to decay power for the tantalum shell. For all of the isotopes that contribute more than 1%, CINDER2008 and CINDER90 are within 5% of each other. The total decay power between the two codes is within 4%.

Table 10. Tantalum Shell Decay Power Contributions after 10 years of Operation

Rank	CINDER90 Isotope	CINDER90 (W)	Percent of Total	CINDER2008 Isotope	CINDER2008 (W)	Percent of Total
1	^{182}Ta	1.0566E+01	96.3652	^{182}Ta	1.1048E+01	96.9417
2	^{183}Ta	1.5660E-01	1.4282	^{183}Ta	1.5571E-01	1.3663
3	^{182m}Ta	5.3106E-02	0.4843	^{176}Ta	1.5363E-02	0.1348
4	^{176}Ta	1.5471E-02	0.1411	^{168}Lu	8.5049E-03	0.0746
5	^{168}Lu	8.5049E-03	0.0776	^{175}Ta	8.2347E-03	0.0723
6	^{178m}Ta	7.7077E-03	0.0703	^{178m}Ta	7.7070E-03	0.0676
7	^{170}Lu	6.9311E-03	0.0632	^{170}Lu	6.9311E-03	0.0608
8	^{172}Lu	5.7714E-03	0.0526	^{172}Lu	5.2113E-03	0.0457
9	^{175}Ta	5.2944E-03	0.0483	^{180}Ta	4.7552E-03	0.0417
10	^{171}Hf	4.6486E-03	0.0424	^{169}Lu	3.9422E-03	0.0346
Top 10 Total		1.0830E+01	98.7733		1.1264E+01	98.8402
Total Decay Power		1.0965E+01			1.1396E+01	

Overall, Table 11 shows that CINDER2008 and CINDER90 are within 24% on the total decay power after 10 years of decay. The relatively large discrepancy between the two codes stems from CINDER90 calculating almost a factor of 2 more ^{148}Gd decay power than CINDER2008, and that CINDER90 calculates a relatively high amount of ^{179}Ta decay power whereas CINDER2008 does not have ^{179}Ta in the top ten contributors.

Table 11. Tantalum Shell Decay Power Contributions after 10 years of Decay

Rank	CINDER90 Isotope	CINDER90 (W)	Percent of Total	CINDER2008 Isotope	CINDER2008 (W)	Percent of Total
1	^{172}Lu	1.0112E-04	36.6664	^{172}Lu	9.1370E-05	40.3582
2	^{148}Gd	8.2069E-05	29.7586	^{148}Gd	4.4722E-05	19.7536
3	^{133}Ba	2.0051E-05	7.2705	^{133}Ba	2.0011E-05	8.8390
4	^{179}Ta	1.6071E-05	5.8275	^{3}H	1.3311E-05	5.8796
5	^{3}H	1.3313E-05	4.8273	^{152}Eu	1.2806E-05	5.6562
6	^{172}Hf	9.3335E-06	3.3844	^{179}Ta	1.0695E-05	4.7240
7	^{152}Eu	9.0924E-06	3.2970	^{172}Hf	7.8432E-06	3.4643
8	^{174}Lu	7.3160E-06	2.6528	^{174}Lu	6.5975E-06	2.9141
9	^{173}Lu	4.3211E-06	1.5669	^{173}Lu	4.6190E-06	2.0402
10	^{178n}Hf	3.9505E-06	1.4325	^{145}Pm	2.9814E-06	1.3169
Top 10 Total		2.6664E-04	96.6839		2.1496E-04	94.9461
Total Decay Power		2.7578E-04			2.2640E-04	

4.2.3 Steel Layer

Figure 15 shows the decay power for the steel layer as calculated by CINDER90 and CINDER2008. Throughout both the operational and decay periods, the two codes are within 3% of each other. The two codes are in good agreement for the steel layer.

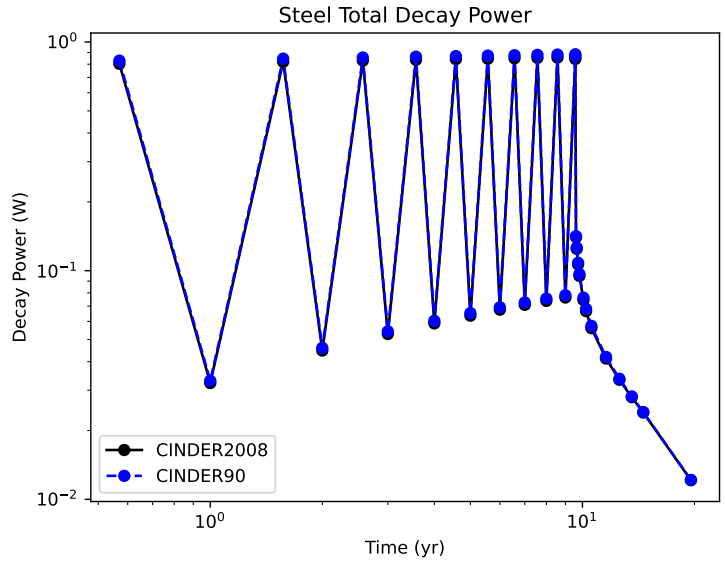

(a) CINDER2008 and CINDER90 decay power over time.

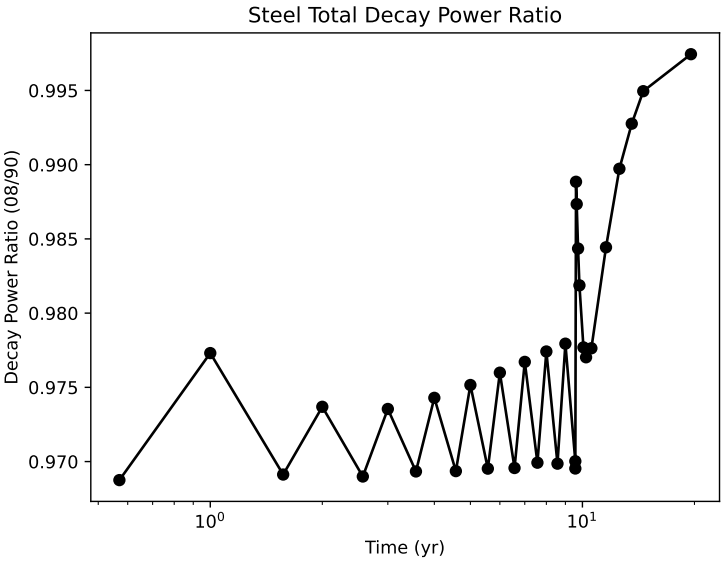

(b) Ratio of CINDER2008 and CINDER90 decay power.

Figure 15. Position-averaged decay power for a single steel layer over time.

Table 12 shows the top contributors to the decay power for the steel layer after 10 years of operation and shows that the two codes are within 10% for the radionuclides that contribute more than 1%.

Table 12. Steel Decay Power Contributions after 10 years of Operation

Rank	CINDER90 Isotope	CINDER90 (W)	Percent of Total	CINDER2008 Isotope	CINDER2008 (W)	Percent of Total
1	^{56}Mn	6.0705E-01	68.6827	^{56}Mn	5.8492E-01	68.2241
2	^{60}Co	4.4740E-02	5.0620	^{60}Co	4.4704E-02	5.2142
3	^{54}Mn	3.3413E-02	3.7804	^{58}Co	3.1982E-02	3.7303
4	^{58}Co	3.1483E-02	3.5621	^{54}Mn	3.0754E-02	3.5871
5	^{52m}Mn	2.1221E-02	2.4010	^{52m}Mn	2.2178E-02	2.5868
6	^{48}V	1.9210E-02	2.1734	^{48}V	1.9414E-02	2.2644
7	^{56}Co	1.4622E-02	1.6544	^{56}Co	1.5596E-02	1.8191
8	^{52}V	1.3829E-02	1.5646	^{52}V	1.3399E-02	1.5628
9	^{52}Mn	1.0108E-02	1.1437	^{52}Mn	9.6734E-03	1.1283
10	^{99}Mo	8.3018E-03	0.9393	^{44}Sc	6.9530E-03	0.8110
Top 10 Total		8.0397E-01	90.9637		7.7957E-01	90.9281
Total Decay Power		8.8384E-01			8.5735E-01	

Table 13 shows ^{60}Co dominating the decay power in both the CINDER2008 and CINDER90 calculations after 10 years of decay. The total decay power calculated by CINDER2008 and CINDER90 are within 0.3% of each other.

Table 13. Steel Decay Power Contributions after 10 years of Decay

Rank	CINDER90 Isotope	CINDER90 (W)	Percent of Total	CINDER2008 Isotope	CINDER2008 (W)	Percent of Total
1	^{60}Co	1.2012E-02	98.8066	^{60}Co	1.2001E-02	98.9715
2	^{55}Fe	3.9057E-05	0.3213	^{55}Fe	3.8494E-05	0.3175
3	^{44}Sc	2.9868E-05	0.2457	^{44}Sc	2.4956E-05	0.2058
4	^{22}Na	2.8406E-05	0.2337	^{63}Ni	2.4003E-05	0.1980
5	^{63}Ni	2.3414E-05	0.1926	^{22}Na	1.4338E-05	0.1182
6	^{54}Mn	1.0030E-05	0.0825	^{54}Mn	9.2317E-06	0.0761
7	^{3}H	7.2047E-06	0.0593	^{3}H	7.2245E-06	0.0596
8	^{42}K	1.9195E-06	0.0158	^{42}K	1.9138E-06	0.0158
9	^{44}Ti	1.6474E-06	0.0136	^{39}Ar	1.4570E-06	0.0120
10	^{39}Ar	1.4608E-06	0.0120	^{44}Ti	1.3724E-06	0.0113
Top 10 Total		1.2155E-02	99.9830		1.2124E-02	99.9858
Total Decay Power		1.2157E-02			1.2126E-02	

4.3 HAZARD CATEGORIZATION COMPARISON

A comparison between CINDER2008 and CINDER90 using the hazard categorization is detailed in this section. The hazard categorization as calculated using the method described in Section 3.6. Section 4.3.1 outlines a comparison between hazard categorization quantities of interest using the same TQs as the First Target Station (FTS) at the SNS (LA-UR-14-20689) and the TQs included in the 2018 DOE Standard 1027 [10, 9]. Section 4.3.2 discusses the hazard categorization results for a single tungsten target wedge.

4.3.1 Threshold Quantities Comparison

Tables 14 & 15 show a comparison of the SORs for each time step as calculated using CINDER90 and CINDER2008 and applying DOE Standard 1027 from 2018 and LA-UR-14-20689 threshold activities for a single tungsten wedge. The time step columns in Tables 14 & 15 shows the incident beam of protons as being either on or off for the duration of the time step. The percent differences in the SORs using DOE Standard 1027 and LA-UR-14-20689 for either CINDER90 or CINDER2008 do not differ by more than 0.4%. The threshold quantities in both references differ for select isotopes but the differences for the isotopes that significantly contribute to the SORs in this analysis are negligible. The last two time steps are not included in these tables due to space constraints and the results closely match time step 30. The discrepancies in the SORs for the decay time steps is due a discrepancy in ^{148} Gd production and destruction and is discussed in detail in Section 4.5.

Table 14. Tungsten Wedge SORs using DOE 1027

Time Step Number	Beam Status	CINDER90	CINDER2008	Percent Difference[a]
1	ON	2.7111E+01	2.7639E+01	-1.9
2	OFF	4.1663E+00	4.1589E+00	0.2
3	ON	2.8478E+01	2.8928E+01	-1.6
4	OFF	5.1840E+00	5.1076E+00	1.5
5	ON	2.9428E+01	2.9759E+01	-1.1
6	OFF	6.0699E+00	5.8661E+00	3.5
7	ON	3.0330E+01	3.0471E+01	-0.5
8	OFF	6.9102E+00	6.5264E+00	5.9
9	ON	3.1188E+01	3.1108E+01	0.3
10	OFF	7.7201E+00	7.1080E+00	8.6
11	ON	3.2019E+01	3.1670E+01	1.1
12	OFF	8.5090E+00	7.6256E+00	11.6
13	ON	3.2832E+01	3.2173E+01	2.0
14	OFF	9.2765E+00	8.0869E+00	14.7
15	ON	3.3636E+01	3.2635E+01	3.1
16	OFF	1.0031E+01	8.5033E+00	18.0
17	ON	3.4422E+01	3.3046E+01	4.2
18	OFF	1.0776E+01	8.8748E+00	21.4
19	ON	3.5192E+01	3.3420E+01	5.3
20	OFF	3.5019E+01	3.3275E+01	5.2
21	OFF	2.4416E+01	2.2297E+01	9.5
22	OFF	2.1694E+01	1.9522E+01	11.1
23	OFF	1.7790E+01	1.5558E+01	14.3
24	OFF	1.5078E+01	1.2811E+01	17.7
25	OFF	1.0756E+01	8.4567E+00	27.2
26	OFF	9.4948E+00	7.1985E+00	31.9
27	OFF	8.4120E+00	6.1261E+00	37.3
28	OFF	7.7978E+00	5.5346E+00	40.9
29	OFF	7.5926E+00	5.3482E+00	42.0
30	OFF	7.4395E+00	5.2139E+00	42.7

[a]Percent Difference = $\frac{\text{CINDER90}-\text{CINDER2008}}{\text{CINDER2008}} \times 100$

Table 15. Tungsten Wedge SORs using LA-UR-14-20689

Time Step Number	Beam Status	CINDER90	CINDER2008	Percent Difference[a]
1	ON	2.7210E+01	2.7738E+01	-1.9
2	OFF	4.1668E+00	4.1594E+00	0.2
3	ON	2.8577E+01	2.9026E+01	-1.5
4	OFF	5.1843E+00	5.1079E+00	1.5
5	ON	2.9527E+01	2.9857E+01	-1.1
6	OFF	6.0702E+00	5.8663E+00	3.5
7	ON	3.0428E+01	3.0569E+01	-0.5
8	OFF	6.9104E+00	6.5266E+00	5.9
9	ON	3.1286E+01	3.1206E+01	0.3
10	OFF	7.7202E+00	7.1080E+00	8.6
11	ON	3.2117E+01	3.1768E+01	1.1
12	OFF	8.5090E+00	7.6255E+00	11.6
13	ON	3.2930E+01	3.2272E+01	2.0
14	OFF	9.2763E+00	8.0868E+00	14.7
15	ON	3.3734E+01	3.2733E+01	3.1
16	OFF	1.0031E+01	8.5031E+00	18.0
17	ON	3.4520E+01	3.3144E+01	4.2
18	OFF	1.0775E+01	8.8745E+00	21.4
19	ON	3.5290E+01	3.3518E+01	5.3
20	OFF	3.5115E+01	3.3372E+01	5.2
21	OFF	2.4471E+01	2.2352E+01	9.5
22	OFF	2.1728E+01	1.9556E+01	11.1
23	OFF	1.7802E+01	1.5571E+01	14.3
24	OFF	1.5082E+01	1.2815E+01	17.7
25	OFF	1.0755E+01	8.4560E+00	27.2
26	OFF	9.4939E+00	7.1976E+00	31.9
27	OFF	8.4111E+00	6.1252E+00	37.3
28	OFF	7.7969E+00	5.5337E+00	40.9
29	OFF	7.5917E+00	5.3473E+00	42.0
30	OFF	7.4387E+00	5.2132E+00	42.7

[a]Percent Difference = $\frac{\text{CINDER90}-\text{CINDER2008}}{\text{CINDER2008}} \times 100$

4.3.2 Tungsten Wedge

Figures 16 & 17 show a direct comparison of the TQ ratios as calculated by CINDER2008 and CINDER90 and provide a overall view of the comparison between CINDER2008 and CINDER90 for the wedge of tungsten directly in the proton beam. The color scheme used in Figures 16 & 17 allows for easy interpretation of the results where the grey color symbolizing the two calculations produced the same amount of the radionuclide, cooler colors (blues) symbolizing CINDER90 calculating more of the radionuclide, and warmer colors (reds) symbolizing CINDER2008 calculating more of the radionuclide. During the operational period, the two calculations agree on the SOR metric but as the decay period begins, CINDER90 tends to predict a higher hazard than CINDER2008. Figure 16 shows the comparison after 10 years of operation.

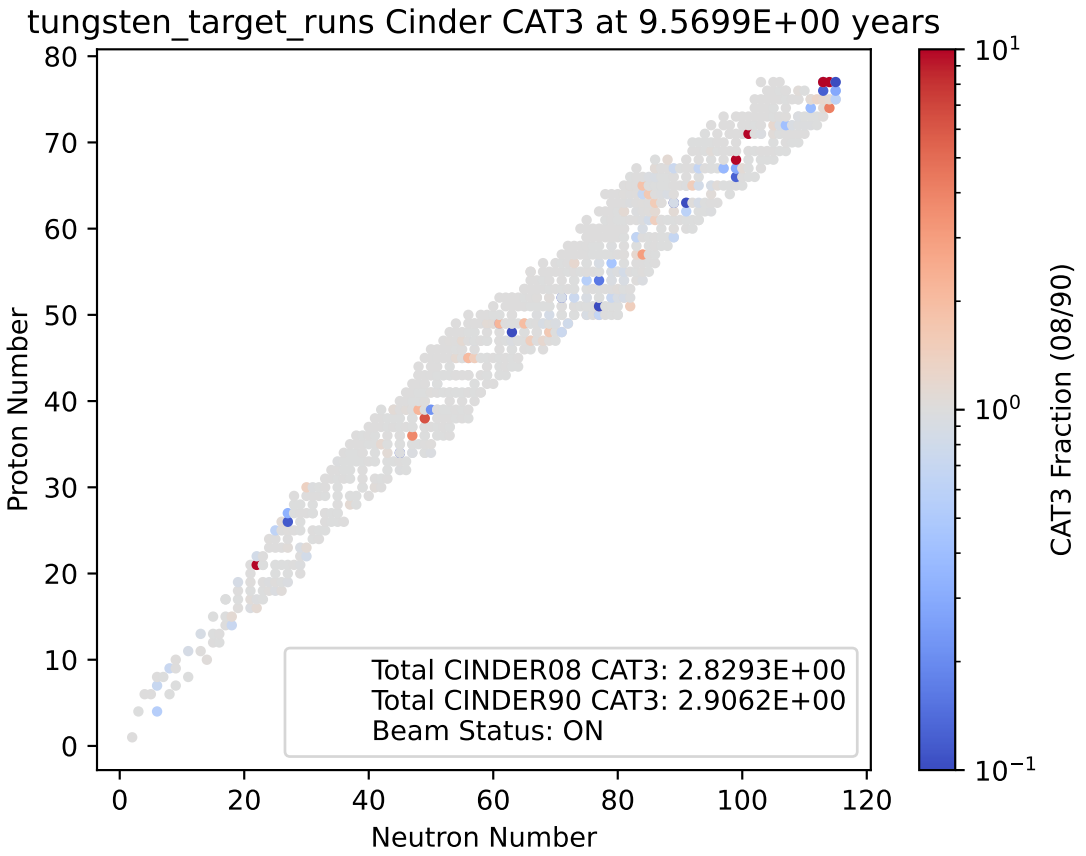

Figure 16. SQ ratios in a ratio of CINDER2008/CINDER90 calculated values for all radionuclides in the initial operational period of 10 years for single tungsten wedge.

Figure 17 shows the SQ ratios directly after a 10 year period of operation followed by a 10 year period of decay.

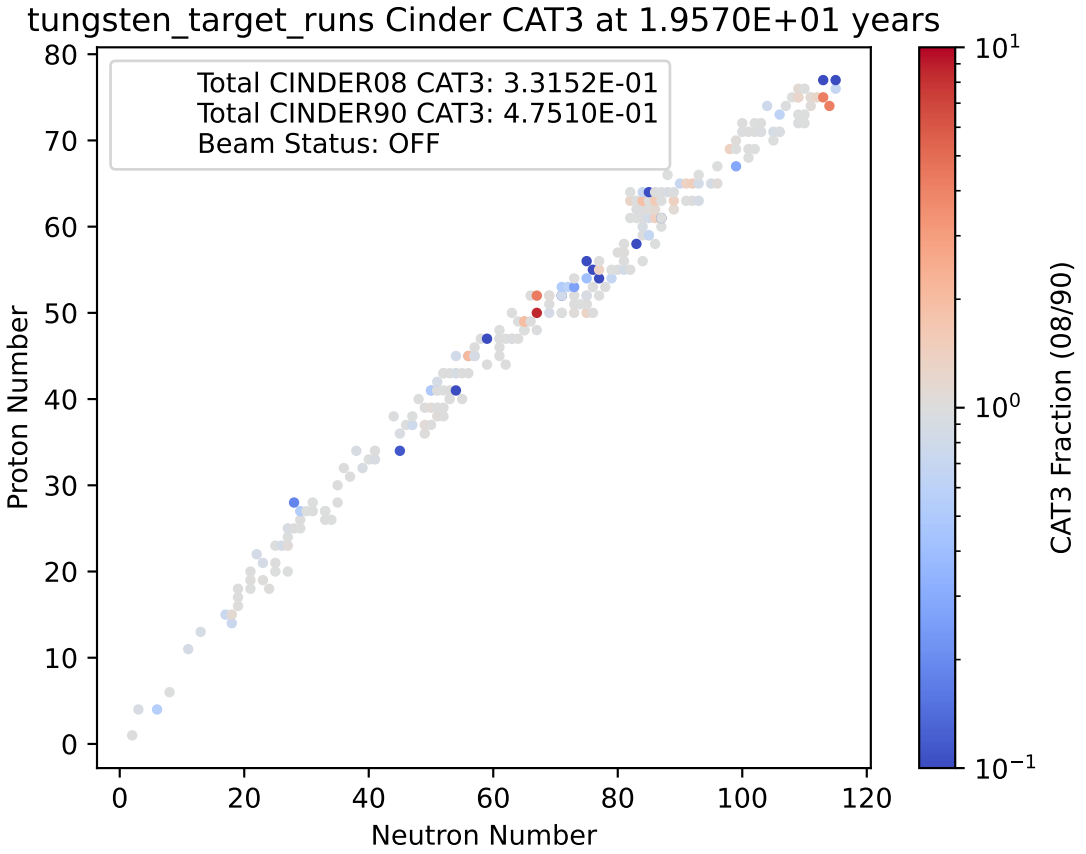

Figure 17. SQ ratios in a ratio of CINDER2008/CINDER90 calculated values for all radionuclides after 10 years of shutdown for a single tungsten wedge.

Tables 16 & 17 show the top contributors to the SOR. After 10 years of operation, ^{125}I dominates the SOR value and after 10 years of cooling down, ^{148}Gd dominates the SOR value. There is a significant difference in the amount of ^{148}Gd produced in the CINDER90 and CINDER2008 calculations. Section 4.5 details a deeper look into the origins of the discrepancy.

Table 16. Tungsten Wedge SOR Contributions after 10 years operation

Rank	CINDER90 Isotope	CINDER90 $\frac{Activity}{TQ}$	Percent of Total	CINDER2008 Isotope	CINDER2008 $\frac{Activity}{TQ}$	Percent of Total
1	^{125}I	2.0915E+01	34.2706	^{125}I	2.0971E+01	35.2953
2	^{187}W	1.2282E+01	20.1238	^{187}W	1.3574E+01	22.8460
3	^{148}Gd	1.0872E+01	17.8136	^{148}Gd	7.5999E+00	12.7912
4	^{185}W	6.3379E+00	10.3850	^{185}W	6.6811E+00	11.2449
5	^{170}Lu	8.7009E-01	1.4257	^{170}Lu	8.7009E-01	1.4644
6	^{176}Ta	7.6657E-01	1.2561	^{176}Ta	7.6657E-01	1.2902
7	^{126}I	7.6427E-01	1.2523	^{126}I	7.6052E-01	1.2800
8	^{124}I	6.5611E-01	1.0751	^{124}I	6.5611E-01	1.1043
9	^{172}Hf	6.2645E-01	1.0265	^{172}Hf	6.2645E-01	1.0544
10	^{172}Lu	5.6725E-01	0.9295	^{172}Lu	5.6726E-01	0.9548
Top 10 Total		5.4657E+01	89.5581		5.3072E+01	89.3256
Total Activity		6.1030E+01			5.9415E+01	

Table 17. Tungsten Wedge SOR Contributions after 10 years shutdown

Rank	CINDER90 Isotope	CINDER90 $\frac{Activity}{TQ}$	Percent of Total	CINDER2008 Isotope	CINDER2008 $\frac{Activity}{TQ}$	Percent of Total
1	^{148}Gd	9.9083E+00	99.3112	^{148}Gd	6.8922E+00	98.9978
2	^{3}H	2.2437E-02	0.2249	^{3}H	2.2437E-02	0.3223
3	^{172}Hf	1.5375E-02	0.1541	^{172}Hf	1.5390E-02	0.2211
4	^{172}Lu	1.1579E-02	0.1161	^{172}Lu	1.1590E-02	0.1665
5	^{133}Ba	7.7825E-03	0.0780	^{133}Ba	7.7878E-03	0.1119
6	^{145}Pm	3.4054E-03	0.0341	^{145}Pm	3.3309E-03	0.0478
7	^{152}Eu	1.8374E-03	0.0184	^{152}Eu	2.5356E-03	0.0364
8	^{179}Ta	8.9948E-04	0.0090	^{178m}Hf	8.6226E-04	0.0124
9	^{90}Sr	7.5042E-04	0.0075	^{90}Sr	7.5096E-04	0.0108
10	^{173}Lu	5.7583E-04	0.0058	^{173}Lu	5.7785E-04	0.0083
Top 10 Total		9.9730E+00	99.9591		6.9574E+00	99.9352
Total Activity		9.9771E+00			6.9619E+00	

4.4 DECAY GAMMA COMPARISON

Comparisons are made for each material separately. The decay gamma metric is the total number of gammas per second per unit volume from the material as it decays over time. In all of the figures, the decay gammas are shown as the sum over all gamma energies and as the sum for gamma energies higher than

500 keV. The sum over energies higher than 500 keV gives a metric to compare the two codes with respect to potential impacts on residual dose rates. The higher energy gammas have a greater impact on effective tissue dose.

Figure 18 shows the decay gamma intensity density for a single tungsten wedge over time. Figure 18b shows the ratio of CINDER2008 over CINDER90 calculated decay gamma intensity. The discrepancies between the two codes when comparing the energy-integrated decay gamma intensity reaches almost a factor of 2 in the "beam on" periods where CINDER90 calculates more decay gammas than CINDER2008. However, the high energy (E_γ >0.5 MeV) discrepancies are only ~5%. With the two codes being in agreement for the high energy gammas, the factor of two discrepancy in the lower energy gammas is unlikely to significantly affect the effective tissue dose when these decay gammas are used as the source to a residual dose calculation.

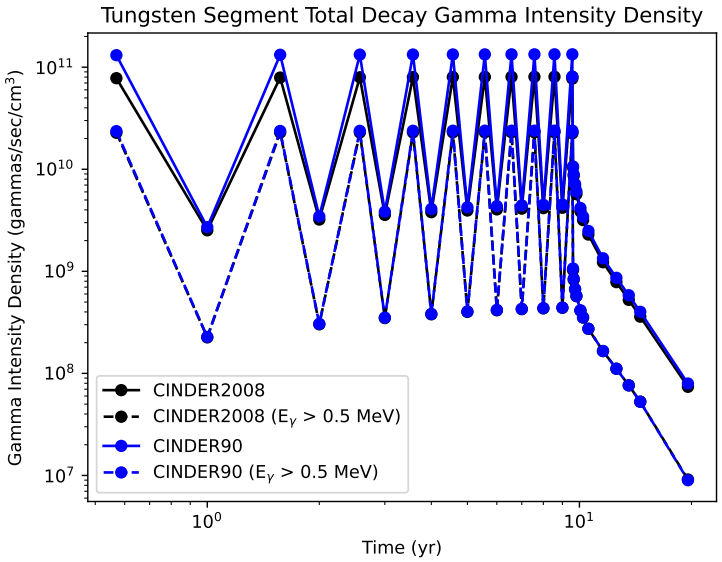

(a) CINDER2008 and CINDER90 decay gamma intensity density over time.

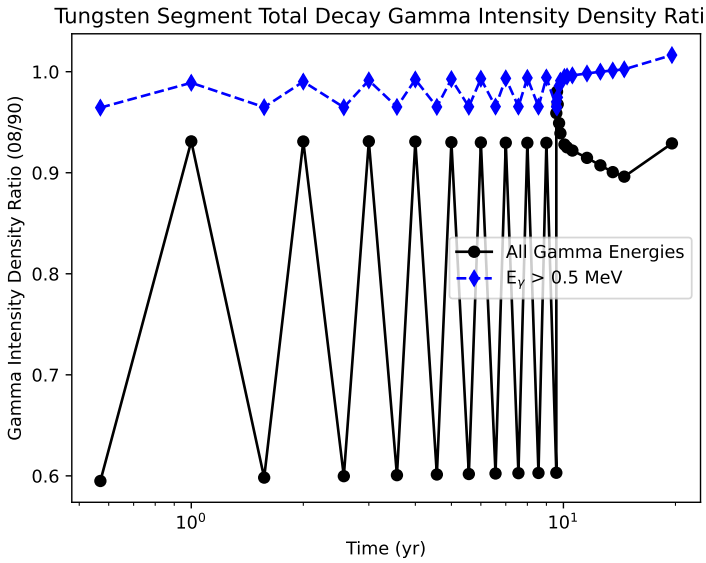

(b) Ratio of CINDER2008 and CINDER90 decay gamma intensity density.

Figure 18. Position-averaged decay gamma intensity density for a single tungsten wedge over time.

Figure 19 shows the total decay gamma intensity over time as calculated by CINDER2008 and CINDER90 along with the ratio of results for the two codes for the tantalum shell. The agreement between the two codes is better for the decay gamma intensity density when compared with the agreement in the tungsten wedge. The discrepancies shown in Figure 19b for the energy integrated decay gamma intensity are no

more than 20%. CINDER2008 consistently over all time steps calculates more high energy decay gammas than CINDER90 but never reaches outside of 5% more. The two codes see the largest discrepancies at the end of the decay period with the two codes being 18% different.

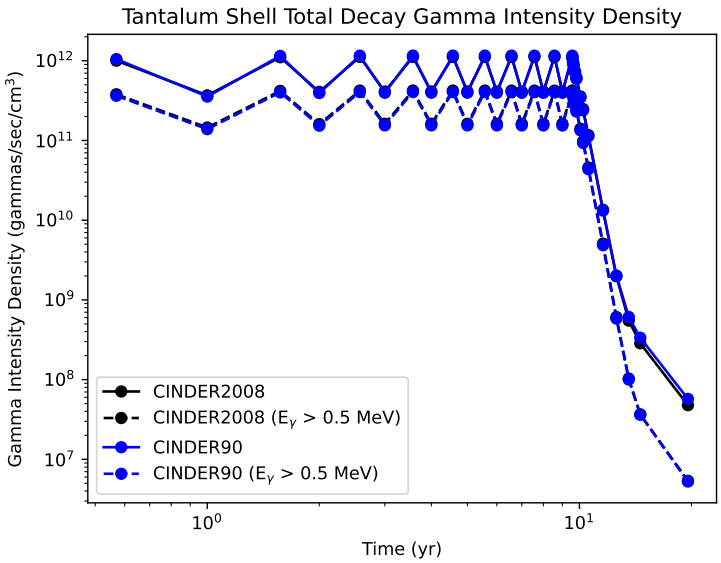

(a) CINDER2008 and CINDER90 decay gamma intensity density over time.

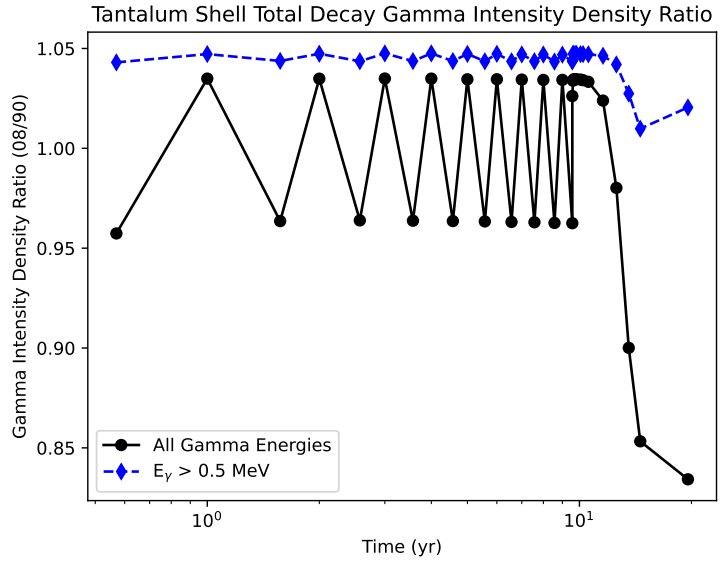

(b) Ratio of CINDER2008 and CINDER90 decay gamma intensity density.

Figure 19. Position-averaged decay gamma intensity density for a single tantalum shell over time.

Figure 20 shows the decay gamma intensity density for the steel layer as calculated by CINDER90 and CINDER2008. Figure 20a shows the energy-integrated and high energy components of the decay gamma intensity. The high energy component contributes much more to the total decay gamma intensity when compared with the tantalum shell and tungsten wedge. Figure 20b shows the ratio between CINDER2008 and CINDER90. The two codes agree to within 7% over all time steps. As the steel layer begins the final decay period, CINDER2008 calculates higher levels of high energy decay gammas when compared with CINDER90.

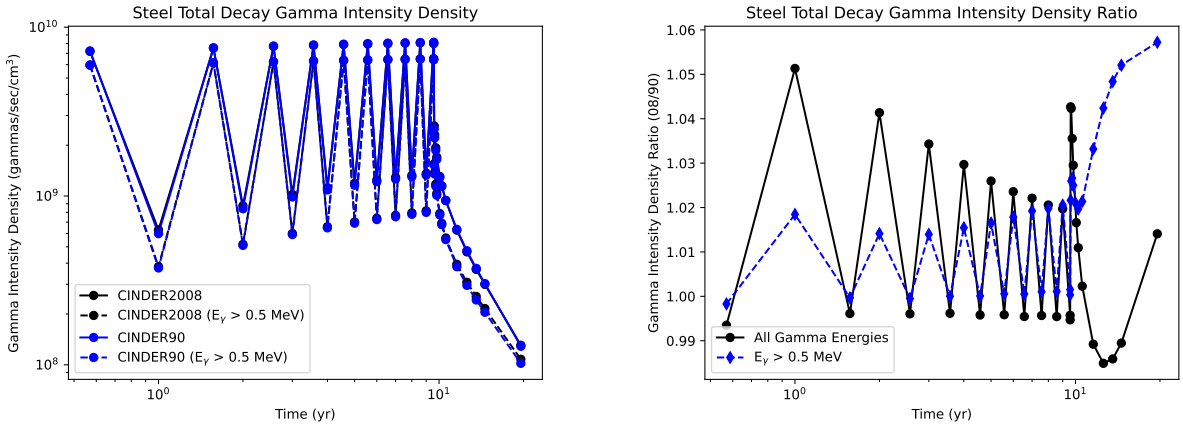

(a) CINDER2008 and CINDER90 decay gamma intensity density over time.

(b) Ratio of CINDER2008 and CINDER90 decay gamma intensity density.

Figure 20. Position-averaged decay gamma intensity density for a single steel layer over time.

4.5 ^{148}GD STUDY

There are some discrepancies in ^{148}Gd results and looks to be a dominant contributor to the decay power, hazard categorization, and potential residual dose. After looking at the cross section data along with the *chains* files from the CINDER calculations, the CINDER90 library does not include many of the destruction mechanisms that are included in the CINDER2008 library. The production mechanisms for ^{148}Gd are similar to within a factor of 2 for both CINDER2008 and CINDER90. Figure 21 shows the atom density of the ^{148}Gd atoms that absorb neutrons and transmute to another isotope as a function of time step number as calculated by CINDER2008 and CINDER90. CINDER2008 calculates the destruction of ^{148}Gd much higher than CINDER90 due to the inclusion of the destructive cross sections that are not in CINDER90's cross section library.

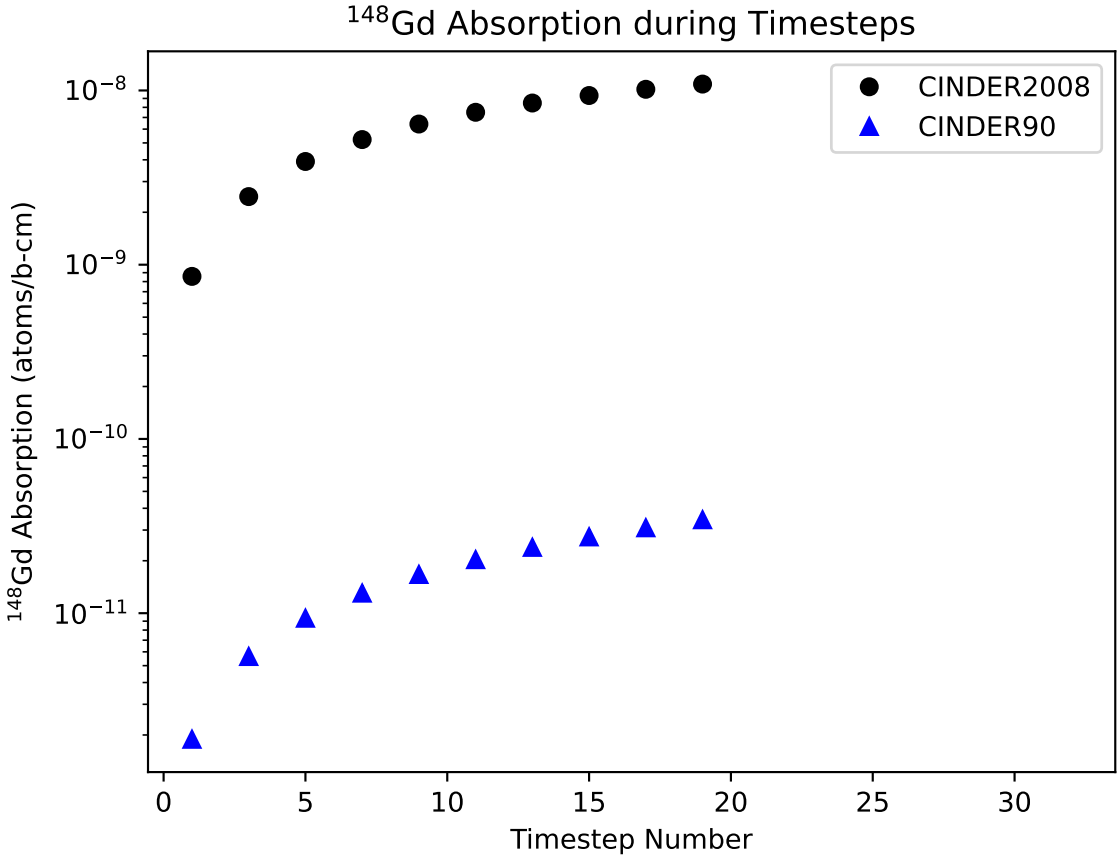

Figure 21. ^{148}Gd destruction over time by ^{148}Gd transmuting to another isotope as calculated by CINDER2008 and CINDER90

Taking a look at the cross sections, Figure 22 shows a comparison of the (n,γ) cross section from a sampling of datasets. There is one measured cross section for ^{148}Gd and the TENDL-2019 cross section passes through this measured cross section at thermal energies as shown in Figure 22 [1].

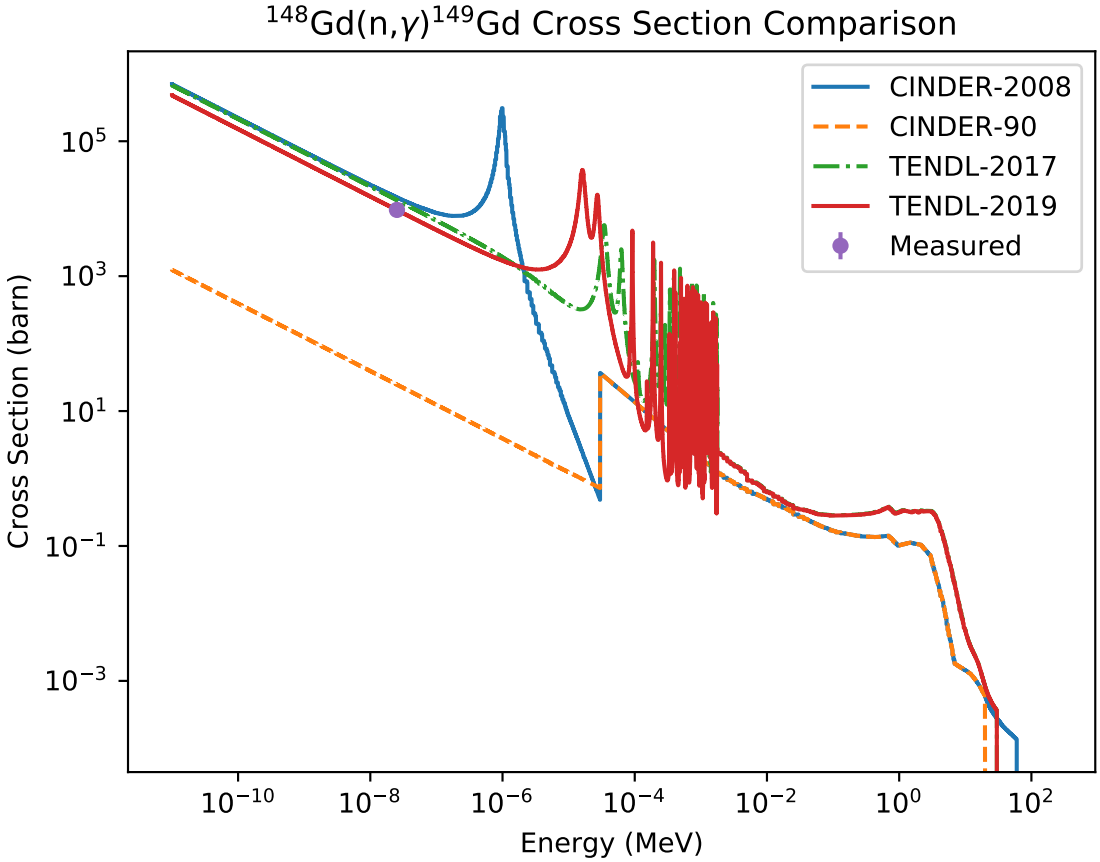

Figure 22. ^{148}Gd(n,γ)^{149}Gd cross section comparison where the measured data are from Rios' measurements [1]

The half lives differ between CINDER90 and CINDER2008 cross section libraries for ^{148}Gd. CINDER2008's cross section library has the half life of ^{148}Gd as 70.947 years whereas CINDER90's cross section library has it as 74.648 years. The difference between these half lives also contributes to a difference in the atom density that accumulates over time. Figure 23 shows the ^{148}Gd atom density that decays each time step. The difference between the CINDER2008 and CINDER90 atom densities increases as time goes along. Prestwood's paper measures the ^{148}Gd half life to be 74.6±3 years [11].

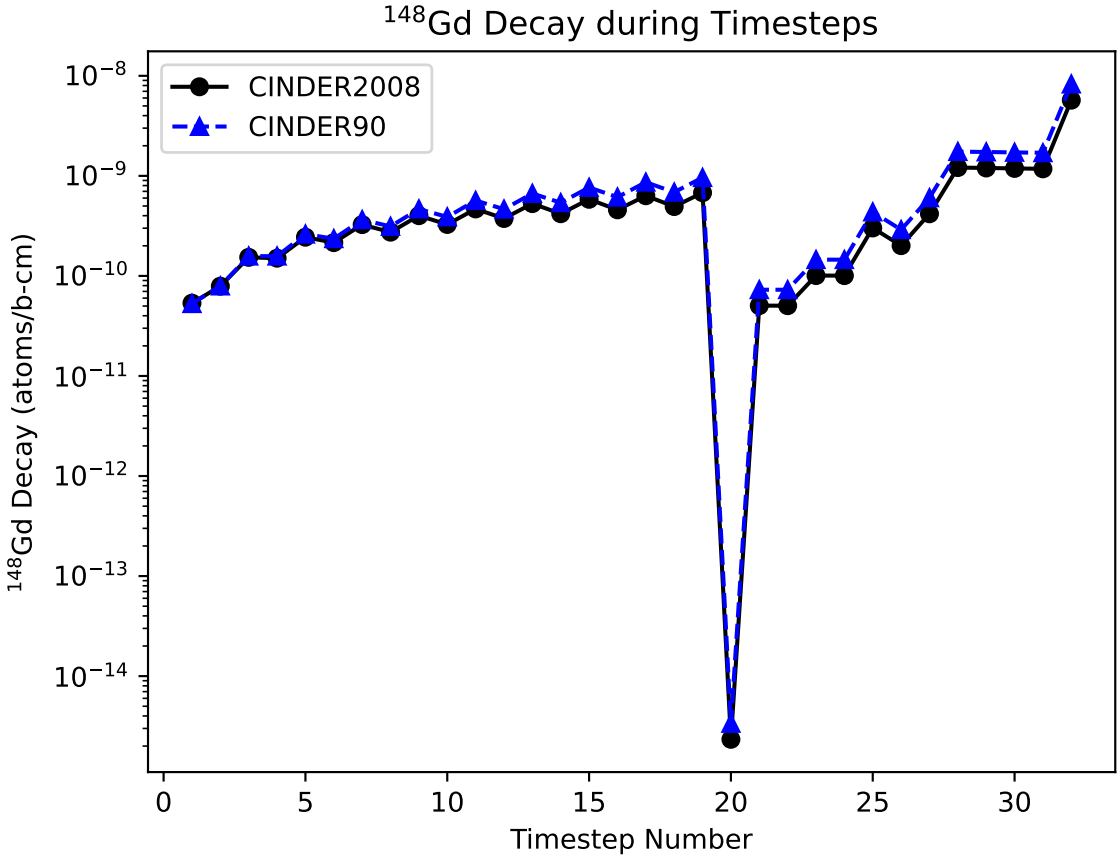

Figure 23. ^{148}Gd destruction over time by ^{148}Gd decaying as calculated by CINDER2008 and CINDER90

4.6 SINGLE VS. MULTIPLE TIME STEPS COMPARISON

This section details a potential bug found in CINDER90 where the number of time steps affects the results of the transmutation calculation.

4.6.1 Methods

The bug in CINDER90 is evaluated with two CINDER90 calculations where one calculation has a single 5 second time step with the beam on and the other calculation has 5, 1 second time steps with the beam on. Both calculations use the same *fluxes*, *splprods*, *material*, and cross section library files. Also, all of the cinder run options are the same in both calculations and the calculations are for the same integral amount of time. The only difference between the two calculations is the number of time steps.

The example calculations used to evaluate the bug are for a steel material exposed to high-energy neutron fluxes on the order of 1×10^{12} n/cm^2/sec along with the spallation products from the 1.3 GeV protons incident on the steel material. These neutron fluxes are used to transmute the original steel material and

spallation products for 5 seconds in both calculations.

4.6.2 Results

The results from the two calculations are discussed in detail in this section along with a comparison between CINDER2008 and CINDER90 running both calculations. CINDER2008 appears to not have the bug. The chain truncation schemes present in CINDER90 were completely re-engineered for CINDER2008, and it is not surprising that the truncation bugs present in CINDER90 were not incorporated in to CINDER2008.

Table 18 shows an overview of the single versus multiple time steps comparison for both CINDER2008 and CINDER90. The totals of the activity, decay power and hazard classification are shown in Table 18 for CINDER2008 are the same for both the single and multiple time step calculations. However, the some of the total figures of merit for CINDER90 change by more than a factor of 7.

Table 18. Single vs. Multiple Time steps Comparison

	CINDER2008		CINDER90	
Attribute	**Single Time Step**	**Long Time Steps**	**Single Time Step**	**Long Time Steps**
Activity (Ci)	6.8690E-01	6.8690E-01	6.5710E-01	6.3950E-01
Decay Power (W)	3.5990E-03	3.5990E-03	3.1650E-03	2.9320E-03
SOR	6.2888E-06	6.2888E-06	5.5996E-06	7.3947E-07

Table 19 shows the top activity contributors for the CINDER2008 runs and shows that the top 10 contributors do not change between the single and multiple time steps runs.

Table 19. CINDER2008 Activity Contributions

	Single Time Step		Long Time Steps	
Rank	**Isotope**	**Activity** (Ci)	**Isotope**	**Activity** (Ci)
1	^{45m}Sc	4.1120E-01	^{45m}Sc	4.1120E-01
2	^{26m}Al	3.3550E-02	^{26m}Al	3.3550E-02
3	^{60m}Co	2.2800E-02	^{60m}Co	2.2800E-02
4	^{46m}Sc	2.0660E-02	^{46m}Sc	2.0660E-02
5	^{27}Si	1.8780E-02	^{27}Si	1.8780E-02
6	^{90m}Zr	1.5140E-02	^{90m}Zr	1.5140E-02
7	^{56}Mn	1.4640E-02	^{56}Mn	1.4640E-02
8	^{52}V	1.3570E-02	^{52}V	1.3570E-02
9	^{24m}Na	1.2610E-02	^{24m}Na	1.2610E-02
10	^{46}V	1.2430E-02	^{46}V	1.2430E-02

Table 20 shows the top 10 contributors to the activity for the CINDER90 calculations and some of the top 10 isotopes are not the same in both calculations. For example, ^{56}Mn is ranks seventh in the single time step run but does not show in the top 10 of the multiple time steps.

Table 20. CINDER90 Activity Contributions

Rank	Single Time Step Isotope	Single Time Step Activity (Ci)	Long Time Steps Isotope	Long Time Steps Activity (Ci)
1	^{45m}Sc	4.1120E-01	^{45m}Sc	4.1120E-01
2	^{26m}Al	3.3130E-02	^{26m}Al	3.3130E-02
3	^{46m}Sc	2.0710E-02	^{46m}Sc	2.0710E-02
4	^{60m}Co	1.9450E-02	^{60m}Co	1.9450E-02
5	^{27}Si	1.8720E-02	^{27}Si	1.8720E-02
6	^{90m}Zr	1.5130E-02	^{90m}Zr	1.5130E-02
7	^{56}Mn	1.3600E-02	^{24m}Na	1.2610E-02
8	^{24m}Na	1.2610E-02	^{46}V	1.2430E-02
9	^{46}V	1.2430E-02	^{54}Co	7.3760E-03
10	^{54}Co	7.3760E-03	^{34}Cl	7.3730E-03

Table 21 shows the isotopes that have the largest differences between the two CINDER90 calculations. These isotopes have been filtered by contributing at least 0.1% to the total activity. There are some minor differences in other isotopes not shown in Table 21 but they do not contribute more than 0.1% to the total activity. The largest observed difference between the single and multiple time steps calculations is with the ^{56}Mn activity with the difference being a factor of approximately 75 between the two calculations. Following the *chains* files produced by following the production and destruction of ^{56}Mn, it appears that the multiple time steps calculation does not include the ^{56}Fe(n,p)^{56}Mn reaction. This (n,p) reaction is a dominant contributor to the single time step calculation and the cross section is at a maximum in the 10 MeV region where the neutron flux magnitude is very high.

Table 21. CINDER90 Activity Differences

Isotope	Half Life (hr)	Single Time Step Activity (Ci)	Long Time Steps Activity (Ci)	Ratio Single/Multiple
^{8}Be	1.9444E-20	1.8450E-03	1.1520E-03	1.60
^{52}V	6.2383E-02	5.8660E-03	5.3000E-03	1.11
^{53}V	2.6667E-02	4.0360E-03	2.7720E-03	1.46
^{55}Cr	5.8283E-02	1.8110E-03	8.4800E-04	2.14
^{56}Mn	2.5789E+00	1.3600E-02	1.8140E-04	74.97

5 CONCLUSIONS

A comparison between CINDER2008 and CINDER90 has been completed using metrics significant to the STS project. A detailed discussion of the model and CINDER options is detailed in the sections above along with a discussion of the activity, decay power and decay gamma intensity density comparisons for several regions of the target assembly. The activity comparison between CINDER90 and CINDER2008 yielded that the total activity between the two codes among any of the parts observed no more than 30% difference. CINDER2008 consistently predicted lower total activities during the “beam on” irradiation

periods when compared with CINDER90. The decay power metric agreed to within 15% between the two codes for tungsten, tantalum, and steel components of the target over all time steps. Decay gamma intensity density saw the largest discrepancies with CINDER90 predicting a factor of ~2 more decay gammas than CINDER2008 for the tungsten wedge during the "beam on" periods. However, the high energy gammas agreed to within 6% for all parts over all time steps. CINDER2008 proved to have a more comprehensive cross section set when compared with CINDER90 as discussed in the ^{148}Gd section. A key issue in CINDER90 has been identified where the code prematurely truncates some radionuclei production chains based on the number of time steps included in the input file as discussed in the Single vs. Multiple Time Steps Comparison section.

6 REFERENCES

[1] M. G. Rios, R. J. Casperson, K. S. Krane, and E. B. Norman, "Neutron capture cross sections of ^{148}Gd and the decay of ^{149}Gd," *Phys. Rev. C*, vol. 74, p. 044302, Oct 2006.

[2] S.-M. Kim and M. H. Kim, "A Study on MCNPX-CINDER90 System for Activation Analysis," in *Transactions of the Korean Nuclear Society Autumn Meeting*, 2014.

[3] C. W. Lee, Y.-O. Lee, M.-Y. Ahn, S. Cho, and D. W. Lee, "Activation analyses for the Korea helium cooled ceramic reflector test blanket module," *Fusion Engineering and Design*, vol. 88, no. 9, pp. 2348 – 2351, 2013. Proceedings of the 27th Symposium On Fusion Technology (SOFT-27); Liège, Belgium, September 24-28, 2012.

[4] M. Fassbender, W. Taylor, D. Vieira, M. Nortier, H. Bach, and K. John, "Proton beam simulation with MCNPX/CINDER'90: Germanium metal activation estimates below 30MeV relevant to the bulk production of arsenic radioisotopes," *Applied Radiation and Isotopes*, vol. 70, no. 1, pp. 72 – 75, 2012.

[5] F. X. . Gallmeier, E. B. Iverson, W. Lu, P. D. Ferguson, S. T. Holloway, C. Kelsey, G. Muhrer, E. J. Pitcher, M. Wohlmuther, and B. J. Micklich, "The CINDER'90 Transmutation Code Package for Use in Accelerator Applications in Combination With MCNPX," in *Proceedings of ICANS XIX, the nineteenth meeting of the International Collaboration on Advanced Neutron Sources*, 2010.

[6] E. Bomboni, N. Cerullo, E. Fridman, G. Lomonaco, and E. Shwageraus, "Comparison among MCNP-based depletion codes applied to burnup calculations of pebble-bed HTR lattices," *Nuclear Engineering and Design*, vol. 240, no. 4, pp. 918 – 924, 2010.

[7] B. J. Micklich, F. X. Gallmeier, and M. Wohlmuther, "Comparison of Selected Codes for Calculating Induced Radioactivity at Accelerator Facilities," *Nuclear Technology*, vol. 168, no. 3, pp. 700–705, 2009.

[8] D. Pelowitz, "MCNPX User's Manual," tech. rep., April 2011.

[9] "Hazard categorization of doe nuclear facilities," 2018.

[10] M. E. Pansoy-Hjelvik, R. F. Sartor, J. A. Hargreaves, T. B. Wheeler, T. L. Foppe, V. L. Peterson, and W. C. Walker, "HC-2/3 Threshold Quantity According to DOE Supplemental Guidance NA-1 SD G 1027," Tech. Rep. LA-UR-14-20689, 2014.

[11] R. J. Prestwood, D. B. Curtis, and J. H. Cappis, "Half-life of ^{148}Gd," *Phys. Rev. C*, vol. 24, pp. 1346–1347, Sep 1981.

APPENDIX A. COMPUTER HARDWARE AND SOFTWARE

APPENDIX A. COMPUTER HARDWARE AND SOFTWARE

The Saturn computing cluster at STS was used to perform the analysis discussed in this report. The cinder/105 and cinder/2008 modules were used to load the appropriate CINDER codes and their corresponding software libraries.

APPENDIX B. LOCATION OF COMPUTATIONAL INPUT AND OUTPUT FILES

APPENDIX B. LOCATION OF COMPUTATIONAL INPUT AND OUTPUT FILES

The location of all of the files used to generate the analysis described in this report are located on the Saturn computing cluster hosted at STS in the following directory:
/home/sts_archive/S.03.12_Neutronics/S.03.12.01_Neutronics_Analysis_Support/S03120100-TRT10000_CINDER_Comparison